
DUEL: Exact Likelihood for Masked Diffusion via Deterministic Unmasking

Gilad Turok¹ Chris De Sa¹ Volodymyr Kuleshov¹

Project Page: <https://giladturok.github.io/duel-project>

Abstract

Masked diffusion models (MDMs) generate text by iteratively selecting positions to unmask and then predicting tokens at those positions. Yet MDMs lack proper perplexity evaluation: the ELBO is a loose bound on likelihood under the training distribution, not the test-time distribution, while generative perplexity requires a biased external model and ignores diversity. To address this, we introduce the DUEL framework, which formalizes *deterministic* position selection, unifying leading MDM sampling strategies. We prove **DUEL admits exact likelihood computation** via a simple algorithm, evaluated under the same position selection used at test time. This **gives MDMs proper perplexity for the first time**—the natural analogue of autoregressive perplexity. With proper perplexity in hand, we revisit key questions about MDMs. **MDMs are substantially better than previously thought**: the MDM-autoregressive perplexity gap shrinks by up to 32% on in-domain data and 82% on zero-shot benchmarks. DUEL enables the first principled comparison of fast, parallel samplers across compute budgets—an analysis impossible with the ELBO and unreliable with generative perplexity—identifying probability margin (Kim et al., 2025a) as a strong default. Finally, oracle search over position orderings reveals MDMs can far surpass autoregressive models—achieving 36.47 vs. 52.11 perplexity on AG News—demonstrating the ceiling of MDM performance has not yet been reached.

1. Introduction

Diffusion models have achieved remarkable success in continuous domains such as images and video (Ho et al., 2020;

¹Department of Computer Science, Cornell University, New York, New York, USA. Correspondence to: Gilad Turok <gt345@cornell.edu>.

Preprint. March 3, 2026.

Song et al., 2020). Recently, masked diffusion models (MDMs) have extended this success to discrete domains (Austin et al., 2021; Sahoo et al., 2024; Shi et al., 2024; Lou et al., 2024), and scaled to billions of parameters with strong results across language benchmarks (Nie et al., 2025; Bie et al., 2025; Labs et al., 2025; Song et al., 2025).

Under the any-order autoregressive (AO-ARM) interpretation (Hoogeboom et al., 2021a; Ou et al., 2024; Kim et al., 2025a), MDM generation decomposes into two components. The unmasking policy π performs *position selection*: it determines which masked positions to reveal. The denoising distribution p_θ , parameterized by a neural network x_θ , performs *token prediction*: given a partially masked sequence, it outputs a probability distribution over tokens at each masked position. Together, these define a complete generative procedure: the policy selects positions, tokens are sampled from the denoiser’s predictions, and this repeats until the full sequence is generated. Figure 1 illustrates one such step.

This decomposition has an important consequence: for a fixed pretrained network x_θ , MDMs define not one generative model but a *family* of models indexed by the choice of policy π . Each policy produces a different collection of samples, implicitly defining a marginal distribution over text sequences.

Notably, many of the best-performing MDM samplers use *deterministic* unmasking policies. Methods like greedy confidence (Nie et al., 2025), probability margin (Kim et al., 2025a), confidence threshold (Wu et al., 2025), and KLASS (Kim et al., 2025b) each define an *unmasking rule* F —a deterministic function mapping partially masked sequences to positions—based on heuristics applied to the network output. Each rule F induces a deterministic unmasking policy π^F with no randomness in position selection.

We introduce the **Deterministic Unmasking Exact Likelihood (DUEL)** framework to formalize and exploit this structure. A DUEL sampler is a pair (x_θ, F) of a denoiser network and a deterministic unmasking rule. We prove that the distribution induced by a DUEL sampler admits exact likelihood computation via a simple algorithm. The key insight: likelihood normally requires marginalizing over all unmasking orderings—a super-exponential sum

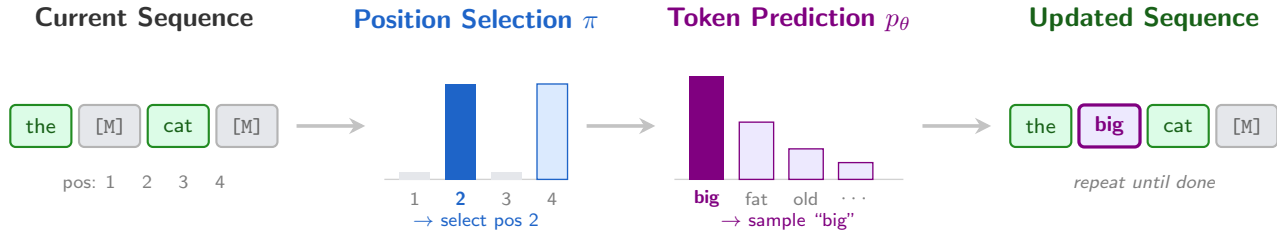


Figure 1. **One step of MDM generation.** Given a partially masked sequence, the unmasking policy π performs *position selection* (choosing position 2), and the denoising network p_θ performs *token prediction* at that position (sampling “big”). This repeats until no masked positions remain.

with $> L!$ terms—but a deterministic policy collapses this to a single term that mirrors the generation procedure.

Perplexity is the standard metric for evaluating language models, measuring the exact probability assigned to text under the generative procedure. However, MDMs currently lack an equivalent. The evidence lower bound (ELBO) is both loose and measures the wrong distribution: it bounds likelihood under *uniform random* position selection π^{unif} used for training, not the deterministic policies π^F often used at test time. Generative perplexity requires an external reference model that is biased and expensive, and ignores sample diversity—a model that repeats one good sentence scores well despite mode collapse. DUEL resolves this: it computes exact likelihood under the test-time distribution induced by π^F , giving MDMs a proper perplexity metric for the first time.

In summary, our contributions are as follows:

- **The DUEL framework.** We formalize DUEL samplers that pair a pretrained denoiser x_θ with a deterministic unmasking rule F . We prove this admits exact likelihood computation (Theorem 4.3), unifying leading MDM sampling strategies under a common probabilistic formalism.
- **Proper MDM perplexity.** We establish DUEL likelihood as the proper perplexity metric for MDMs—the natural analogue of autoregressive perplexity—measuring the test-time distribution directly and avoiding the shortcomings of the ELBO and generative perplexity.
- **Reassessing the perplexity gap.** Across multiple models and datasets, DUEL likelihood reveals that MDMs are substantially closer to autoregressive models than the ELBO suggests, reducing the perplexity gap by up to 32% on in-domain test data and 82% on zero-shot benchmarks.
- **Comparing sampling strategies.** DUEL enables principled comparison of sampling strategies that is impossible with the ELBO and unreliable with generative perplexity. Fast parallel samplers can be reliably ranked across compute budgets, identifying probability margin (Kim et al., 2025a) as a strong default. Oracle search over orderings

reveals MDMs can far surpass autoregressive baselines—36.47 vs. 52.11 perplexity on AG News—by exploiting flexibility in generation order that ARMs cannot match.

2. Background

We briefly review masked diffusion models (MDMs) for language generation (Austin et al., 2021; Sahoo et al., 2024; Shi et al., 2024; Lou et al., 2024; Gat et al., 2024; Nie et al., 2025). See Section B.1 for extended MDM details.

Forward Process. MDMs define a forward process that progressively masks a clean sequence $\mathbf{x} = (x^{(1)}, \dots, x^{(L)}) \in \mathcal{V}^L$ over time $t \in [0, 1]$, where $\mathcal{V} = \{1, \dots, V\}$ is a vocabulary of V tokens. Each position independently either retains its value or transitions to a special mask token \mathfrak{m} :

$$q_{t|0}(z^{(\ell)} | x^{(\ell)}) = \text{Cat}(\alpha_t \mathbf{e}_{x^{(\ell)}} + (1 - \alpha_t) \mathbf{e}_{\mathfrak{m}}),$$

where \mathbf{e}_v is the one-hot vector for token v . The noise schedule satisfies $\alpha_0 = 1$ (clean) and $\alpha_1 = 0$ (fully masked). The mask token is *absorbing*: once masked, a position remains masked, yielding partially masked sequences $\mathbf{z} \in \mathcal{V} \cup \{\mathfrak{m}\}$.

Reverse Process. Generation reverses this corruption: starting from a fully masked sequence, the model iteratively predicts and reveals tokens at masked positions $\mathcal{M}(\mathbf{z}) = \{\ell : z_\ell = \mathfrak{m}\}$. A *denoising network* x_θ takes a partially masked sequence \mathbf{z} and outputs logits predicting clean tokens at each position. We define the token probability matrix $\mathbf{P} = \text{softmax}(x_\theta(\mathbf{z})) \in \Delta_V^L$, where each row P_ℓ is a distribution over tokens at position ℓ . The reverse transition substitutes these predictions for the unknown ground truth: $p_\theta(z_s^{(\ell)} | \mathbf{z}_t) = q_{s|t}(z_s^{(\ell)} | \mathbf{z}_t, \mathbf{x} \leftarrow \mathbf{P})$.

Training Objective. The data likelihood marginalizes over latent masked trajectories, $p_\theta(\mathbf{x}) = \sum_{\mathbf{z}_{0:T}} p_\theta(\mathbf{x}, \mathbf{z}_{0:T})$, which is intractable. Following Sahoo et al. (2024), we obtain a tractable ELBO that reduces to the expected negative

log-likelihood of true tokens at masked positions:

$$\mathcal{L}_{\text{ELBO}}(\theta) = \mathbb{E}_{\substack{t \sim \text{Unif}[0,1] \\ \mathbf{z}_t \sim q_{t|0}(\cdot|\mathbf{x})}} \left[w_t \sum_{\ell \in \mathcal{M}(\mathbf{z}_t)} -\log p_{\theta}(x^{(\ell)} | \mathbf{z}_t) \right], \quad (1)$$

where $w_t = \alpha'_t / (1 - \alpha_t)$ weights each timestep according to the noise schedule derivative.

AO-ARM Interpretation. MDMs admit an equivalent interpretation as any-order autoregressive models (AO-ARMs) (Uria et al., 2014; Yang et al., 2019; Hoogeboom et al., 2021a), decomposing generation into *position selection* via an unmasking policy π_{θ} and *token prediction* via a denoising distribution p_{θ} . Recent work formally establishes that the MDM training loss of Equation (1) is equivalent to the AO-ARM ELBO of Equation (5): both reduce to the expected negative log-likelihood of true tokens at masked positions, averaged over random orderings (Zheng et al., 2024; Ou et al., 2024; Kim et al., 2025a). We adopt and extend this perspective in Section 4.

3. The DUEL Framework

We introduce DUEL samplers—pairs of a denoiser network and an unmasking rule—that define implicit generative procedures over sequences. Section 3.1 defines these components and shows how they enable sampling. Section 3.2 presents common instantiations of unmasking rules.

3.1. DUEL Samplers

A DUEL sampler combines two components: a denoising network that predicts tokens, and an unmasking rule that selects positions. In practice, this is just a pretrained MDM together with a choice of how to sample from it.

Definition 3.1 (Unmasking Rule). An *unmasking rule* F is a deterministic function mapping a partially-revealed sequence \mathbf{z} to a non-empty subset of masked positions:

$$\emptyset \neq F(\mathbf{z}) \subseteq \mathcal{M}(\mathbf{z}).$$

Since the token probabilities $\mathbf{P} = \text{softmax}(x_{\theta}(\mathbf{z}))$ are deterministic functions of \mathbf{z} , rules depending on \mathbf{P} are valid. The non-emptiness constraint ensures generation progresses at each step.

Definition 3.2 (DUEL Sampler). A DUEL *sampler* is a pair (x_{θ}, F) of a pretrained denoising network x_{θ} outputting token probabilities $\mathbf{P} = \text{softmax}(x_{\theta}(\mathbf{z}))$, and an unmasking rule F selecting which positions to reveal. Each rule F induces a deterministic unmasking policy π^F , formalized in Section 4.1, that places all probability mass on the positions F selects.

A DUEL sampler defines an *implicit* generative procedure: we can draw samples without ever writing down the induced

Table 1. Unmasking rules defining deterministic policies. $\mathcal{M} = \mathcal{M}(\mathbf{z})$ denotes masked positions; $\mathbf{P} = \text{softmax}(x_{\theta}(\mathbf{z}))$ is the token probability matrix.

Unmask Rule F	Selected Positions $F(\mathbf{z})$
Left-to-Right	$\{k \text{ smallest } \ell : z_{\ell} = \mathbf{m}\}$
Greedy Conf.	$\arg \max_{ \mathcal{I} =k} \sum_{\ell \in \mathcal{I}} P_{\ell}^{(1)}$
Prob. Margin	$\arg \max_{ \mathcal{I} =k} \sum_{\ell \in \mathcal{I}} (P_{\ell}^{(1)} - P_{\ell}^{(2)})$
Conf. Thresh.	$\{\ell \in \mathcal{M} : P_{\ell}^{(1)} \geq \mu\}$
KLASS	$\{\ell \in \mathcal{M} : P_{\ell}^{(1)} \geq \mu, \text{KL}(\hat{P}_{\ell} \ P_{\ell}) \leq \nu\}$

distribution in closed form. Starting from the fully masked sequence, we repeatedly: (1) compute token distributions via the denoising network, (2) select positions deterministically via F , and (3) sample and reveal tokens at those positions. Generation terminates when all positions are unmasked. Algorithm 1 formalizes this procedure.

3.2. Instantiations

The DUEL framework unifies leading MDM generation strategies: each corresponds to an unmasking rule F inducing a deterministic policy π^F with exact likelihood via Theorem 4.3. We write $P_{\ell}^{(1)}$ and $P_{\ell}^{(2)}$ for the highest and second-highest token probabilities at position ℓ ; see Table 1.

Left-to-Right. Unmask the k smallest masked indices, recovering autoregressive generation when $k = 1$.

Greedy Confidence. (Nie et al., 2025). Select the k positions with highest predicted confidence $P_{\ell}^{(1)}$, committing first to tokens where the denoiser is most certain.

Probability Margin (Kim et al., 2025a). Select the k positions with largest gap $P_{\ell}^{(1)} - P_{\ell}^{(2)}$ between top-two predictions, preferring genuine certainty over uniformly high confidence.

Confidence Threshold (Wu et al., 2025). Unmask all positions where $P_{\ell}^{(1)} \geq \mu$, with fallback to the most confident position if none exceed μ . This enables adaptive parallelism—more positions are unmasked when the model is confident.

KLASS (Kim et al., 2025b). Unmask positions that are both confident ($P_{\ell}^{(1)} \geq \mu$) and stable across consecutive steps ($\text{KL}(\hat{P}_{\ell} \| P_{\ell}) \leq \nu$, where \hat{P}_{ℓ} is the previous prediction), with fallback to the most confident position.

Integration with Hybrid Strategies. These rules compose with broader MDM strategies. For *block diffusion models* (Arriola et al., 2025a), any rule F applies independently

within blocks of L' positions while blocks are processed autoregressively. For *entropy-bounded sampling* (Ben-Hamu et al., 2025), the entropy-based selection is a deterministic function of \mathbf{z} . In both cases, any rule that deterministically maps $\mathbf{z} \mapsto \mathcal{I}$ admits exact likelihood computation.

4. Exact Likelihood Computation

A DUEL sampler (x_θ, F) generates samples via Algorithm 1, but what distribution does it sample from? Section 4.1 develops the formulation needed to make this distribution explicit, and Section 4.2 proves that deterministic unmasking enables its exact likelihood computation.

4.1. Any-Order Autoregressive Formulation

Building on the AO-ARM interpretation of MDMs (Section 2), we introduce *ordered partitions* for parallel unmasking and formalize *deterministic unmasking policies*. See Section B.2 for extended details.

Ordered Partitions. We formalize the progression of unmasking steps during generation of target sequence $\mathbf{x} \in \mathcal{V}^L$.

Definition 4.1 (Ordered Partition). An *ordered partition* of positions $[L] = \{1, \dots, L\}$ is a tuple $\sigma = (\sigma_1, \dots, \sigma_T)$ of non-empty subsets satisfying:

$$\bigcup_{t=1}^T \sigma_t = [L], \quad \sigma_t \cap \sigma_{t'} = \emptyset.$$

Each $\sigma_t \subseteq [L]$ is the set of positions unmasked at step t , and T denotes the number of steps, which may depend on \mathbf{x} .

Ordered partitions capture both sequential and parallel unmasking—a distinguishing feature of MDMs over ARMs. When each part is a singleton ($|\sigma_t| = 1$), we recover *sequential unmasking* with $T = L$ steps; when parts contain multiple positions, we obtain *parallel unmasking* with $T < L$ steps. We write $\sigma_{<t} \triangleq \sigma_1 \cup \dots \cup \sigma_{t-1}$ for the set of positions revealed before step t , $\mathbf{x}^{\sigma_{<t}} \triangleq \{x^{(\ell)}\}_{\ell \in \sigma_{<t}}$ for the clean tokens at those positions, and $\mathbf{x}^{\sigma_t} \triangleq \{x^{(\ell)}\}_{\ell \in \sigma_t}$ for the clean tokens revealed at step t itself. Figure 2 illustrates a concrete example.

Joint Factorization. The joint probability of generating sequence \mathbf{x} via ordered partition σ factorizes into position selection and token prediction at each step (derived in Section C.1):

$$p_\theta(\mathbf{x}, \sigma) = \prod_{t=1}^T \underbrace{\pi_\theta(\sigma_t | \mathbf{x}^{\sigma_{<t}})}_{\text{position selection}} \cdot \underbrace{p_\theta(\mathbf{x}^{\sigma_t} | \mathbf{x}^{\sigma_{<t}})}_{\text{token prediction}}, \quad (2)$$

where the *unmasking policy* $\pi_\theta(\sigma_t | \mathbf{x}^{\sigma_{<t}})$ selects which masked positions to reveal conditioned on the revealed tokens, and the *denoising distribution* $p_\theta(\mathbf{x}^{\sigma_t} | \mathbf{x}^{\sigma_{<t}})$ gives

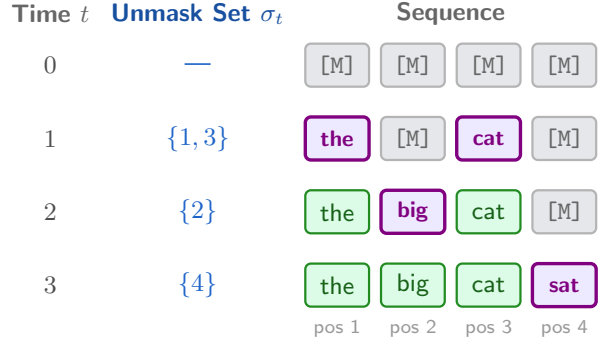


Figure 2. **Unmasking trajectory for $\sigma = (\{1, 3\}, \{2\}, \{4\})$.** Starting from a fully masked sequence ($t=0$), positions are progressively revealed according to the ordered partition. At $t=1$, positions 1 and 3 are unmasked in parallel; subsequent steps unmask one position each.

the probability of tokens at those positions. Under conditional independence (Theorem C.1), the denoising distribution factorizes over positions:

$$p_\theta(\mathbf{x}^{\sigma_t} | \mathbf{x}^{\sigma_{<t}}) = \prod_{\ell \in \sigma_t} p_\theta(x^{(\ell)} | \mathbf{x}^{\sigma_{<t}}),$$

where $p_\theta(x^{(\ell)} | \mathbf{x}^{\sigma_{<t}}) \triangleq P_\ell[x^{(\ell)}]$ with token probabilities $\mathbf{P} = \text{softmax}(x_\theta(\cdot))$ for token $x^{(\ell)}$ at position ℓ .

Deterministic Unmasking Policies. An unmasking rule F induces a *deterministic unmasking policy* π_θ^F that places all probability mass on the positions returned by F :

$$\pi_\theta^F(\sigma_t | \mathbf{x}^{\sigma_{<t}}) = \begin{cases} 1 & \text{if } \sigma_t = F(\mathbf{x}^{\sigma_{<t}}) \\ 0 & \text{otherwise.} \end{cases} \quad (3)$$

Here σ_t ranges over all possible subsets of masked positions, and π_θ^F is a Dirac delta concentrating on the unique subset $F(\mathbf{x}^{\sigma_{<t}})$. Since F is a function, position selection is entirely deterministic given the revealed tokens. The dependence on θ is indirect: F selects positions based on the network’s token probabilities $\mathbf{P} = \text{softmax}(x_\theta(\cdot))$.

Induced Distribution. An AO-ARM defines the data likelihood by marginalizing over ordered partitions: $p_\theta(\mathbf{x}) = \sum_\sigma p_\theta(\mathbf{x}, \sigma)$. Specializing Equation (2) to the deterministic policy π_θ^F yields the distribution induced by a DUEL sampler:

$$p_\theta^{\pi^F}(\mathbf{x}) = \sum_\sigma \prod_{t=1}^T \pi_\theta^F(\sigma_t | \mathbf{x}^{\sigma_{<t}}) \cdot p_\theta(\mathbf{x}^{\sigma_t} | \mathbf{x}^{\sigma_{<t}}). \quad (4)$$

This is the distribution that Algorithm 1 samples from. Crucially, this equation is only made explicit in the AO-ARM formulation of MDMs, and not in the standard *latent-variable* formulation.

Algorithm 1 DUEL: Sampling

Require: Denoiser network x_θ , unmasking rule F
Ensure: Generated sequence \mathbf{x}
 1: $\mathbf{z} \leftarrow (m, \dots, m)$ \triangleright Start fully masked
 2: **while** $\mathcal{M}(\mathbf{z}) \neq \emptyset$ **do**
 3: $\mathbf{P} \leftarrow \text{softmax}(x_\theta(\mathbf{z}))$ \triangleright Token probabilities
 4: $\mathcal{I} \leftarrow F(\mathbf{z})$ \triangleright Positions to unmask
 5: **for** $\ell \in \mathcal{I}$ **do**
 6: $x_\ell \sim \text{Cat}(P_\ell)$ \triangleright Sample token
 7: $\mathbf{z}[\ell] \leftarrow x_\ell$ \triangleright Reveal token
 8: **return** \mathbf{x}

Algorithm 2 DUEL: Exact Likelihood

Require: Sequence \mathbf{x} , denoiser network x_θ , unmasking rule F
Ensure: Log-likelihood $\log p_\theta^{\pi^F}(\mathbf{x})$
 1: $\mathbf{z} \leftarrow (m, \dots, m)$, $\mathbf{ll} \leftarrow 0$ \triangleright Start fully masked
 2: **while** $\mathcal{M}(\mathbf{z}) \neq \emptyset$ **do**
 3: $\mathbf{P} \leftarrow \text{softmax}(x_\theta(\mathbf{z}))$ \triangleright Token probabilities
 4: $\mathcal{I} \leftarrow F(\mathbf{z})$ \triangleright Positions to unmask
 5: **for** $\ell \in \mathcal{I}$ **do**
 6: $\mathbf{ll} \leftarrow \mathbf{ll} + \log P_\ell[x_\ell]$ \triangleright Accumulate
 7: $\mathbf{z}[\ell] \leftarrow x_\ell$ \triangleright Reveal token
 8: **return** \mathbf{ll}

Figure 3. DUEL sampling and exact likelihood computation. Highlights mark the only differences. Both algorithms iterate with a denoising network x_θ and unmasking rule F : compute token probabilities $\mathbf{P} = \text{softmax}(x_\theta(\mathbf{z}))$, select positions via $F(\mathbf{z})$, then either sample tokens or accumulate log-probabilities. Section 4 proves that Algorithm 2 computes the exact likelihood under the distribution induced by F .

Computing Equation (4) directly appears intractable: the sum ranges over all ordered partitions σ , each corresponding to a different generation trajectory. The number of such partitions is super-exponential in the sequence length L . Since the denoiser conditions on different contexts under different orderings, each term in the sum requires separate neural network evaluation. Section 4.2 shows that determinism makes this tractable.

Connection to MDM Training. The MDM–AO–ARM connection becomes precise through the unmasking policy. Under *uniform random* position selection, for a partially masked sequence \mathbf{z} ,

$$\pi^{\text{unif}}(\sigma_t | \mathbf{z}) = \frac{1}{|\mathcal{M}(\mathbf{z})|},$$

each masked position is equally likely to be unmasked next. This policy arises naturally from ancestral sampling of the MDM reverse process: since the forward process independently masks each position at a random time, reversing this process treats all masked positions symmetrically.

Under uniform position selection π^{unif} with *sequential* unmasking (one token per step), the proposal $q(\sigma) = 1/L!$ over permutations yields a tractable ELBO (see Theorems C.3 and C.4 for derivations):

$$\mathcal{L}_{\text{ELBO}}(\theta) = \mathbb{E}_{q(\sigma)} \left[\sum_{t=1}^T \sum_{\ell \in \sigma_t} -\log p_\theta(x^{(\ell)} | \mathbf{x}^{\sigma_{<t}}) \right]. \quad (5)$$

Ou et al. (2024); Kim et al. (2025a) show this is equivalent to the standard MDM loss of Equation (1), formally establishing MDMs as AO-ARMs trained under uniform random ordering. The ELBO serves as a training objective and is widely used for MDM evaluation; however, it does not yield

proper perplexity under the test-time distribution. Section 5 develops this argument.

4.2. Theoretical Results

We establish two results: different unmasking rules induce genuinely different distributions, and deterministic rules enable exact likelihood computation.

Policy-Dependent Distributions. Equation (4) defines the distribution $p_\theta^{\pi^F}$ induced by a DUEL sampler (x_θ, F) . A single denoising network x_θ does not define one generative model—it defines a *family* of distributions $\{p_\theta^{\pi^F} : F \in \mathcal{F}\}$, one for each unmasking rule. Choosing a rule is not merely a computational convenience; it determines which distribution we sample from.

Theorem 4.2 (Policy-Dependent Distribution). *If the denoising network x_θ is order-sensitive—its predictions at masked positions depend on revealed context—then there exist unmasking rules F_1, F_2 inducing different distributions: $p_\theta^{\pi^{F_1}} \neq p_\theta^{\pi^{F_2}}$. (Proof in Section C.4.)*

Exact Likelihood Computation. Computing $p_\theta^{\pi^F}(\mathbf{x})$ from Equation (4) appears to require summing over super-exponentially many ordered partitions. Determinism eliminates this burden. Given any partially masked sequence \mathbf{z} , the rule $F(\mathbf{z})$ outputs a unique set of positions—there is no randomness, so only one choice is possible. Any ordered partition that deviates from what F would select receives zero probability under π_θ^F . And once a token is revealed, it stays revealed, so the partial sequence at each step is fully determined by the input \mathbf{x} . This means exactly one ordered partition σ^* is consistent with the policy, collapsing Equation (4) to a single term.

Theorem 4.3 (DUEL Exact Likelihood). *Let (x_θ, F) be a*

DUEL sampler. Algorithm 2 computes $\log p_{\theta}^{\pi^F}(\mathbf{x})$ exactly, implementing:

$$\log p_{\theta}^{\pi^F}(\mathbf{x}) = \sum_{t=1}^T \sum_{\ell \in \sigma_t^*} \log p_{\theta}(x^{(\ell)} \mid \mathbf{x}^{\sigma_{<t}^*}), \quad (6)$$

where $\sigma^* = (\sigma_1^*, \dots, \sigma_T^*)$ is the unique ordered partition satisfying $\sigma_t^* = F(\mathbf{x}^{\sigma_{<t}^*})$ at each step. (Proof in Theorem C.8.)

Likelihood Follows Generation. This is the crux of DUEL: the likelihood computation follows the same path as generation, simulating the unmasking process but revealing true tokens instead of sampling them. Algorithm 2 implements this procedure.

5. Evaluation via DUEL

Autoregressive perplexity—computed from exact likelihood under the model’s generation procedure—is the standard intrinsic metric for language models. MDMs lack an equivalent: the ELBO is a loose bound on likelihood under the wrong distribution (Section 5.1), and generative perplexity requires a biased external model and ignores diversity (Section 5.2). Neither evaluates the induced generative distribution $p_{\theta}^{\pi^F}(\mathbf{x})$ of Equation (4)—the distribution practitioners actually sample from at test time. DUEL fills this gap, providing proper perplexity for MDMs: exact likelihood under the test-time distribution, evaluated on held-out text. Section 5.3 describes the new experiments this enables and discusses limitations.

5.1. Limitations of the ELBO

The ELBO has two problems as an evaluation tool:

1. **Looseness.** The variational gap $\log p_{\theta}^{\pi^{\text{unif}}}(\mathbf{x}) - (-\mathcal{L}_{\text{ELBO}})$ can be substantial, systematically underestimating model quality.
2. **Wrong distribution.** Even if the bound were tight, the ELBO measures $p_{\theta}^{\pi^{\text{unif}}}$, not the test-time distribution $p_{\theta}^{\pi^F}$ under deterministic policies.

DUEL resolves both: it computes *exact* likelihood under the *test-time* distribution $p_{\theta}^{\pi^F}$.

5.2. Limitations of Generative Perplexity

Generative perplexity—the standard sample-based metric for MDMs—draws samples from the model and scores them under an external reference model, typically GPT-2 (Radford et al., 2019). It has two fundamental limitations:

1. **Reference model dependence.** Scores reflect the reference model’s biases as much as the MDM’s quality (Wang et al., 2024), and running a separate model is expensive at scale.
2. **Ignores diversity.** A model that repeats the same high-quality phrase achieves excellent generative perplexity despite catastrophic mode collapse.

DUEL sidesteps both issues: it requires only the MDM itself, and it evaluates on held-out text, which requires modeling the full data distribution.

Post-hoc Fixes. Others have proposed patches: entropy measures sample diversity as a secondary check, while MAUVE (Pillutla et al., 2021) compares generated and reference text distributions. But entropy is a post-hoc diagnostic that forces practitioners to track two metrics without guidance on reconciling them, and MAUVE inherits the same reference-model bias and is sensitive to hyper-parameters. In general, sample-based evaluation is best reserved for when exact likelihood is unavailable or perplexity does not capture the quality we aim to measure.

5.3. What DUEL Enables

The ELBO is sensitive to the denoiser x_{θ} but ignores the unmasking policy F ; generative perplexity is sensitive to both but relies on a biased reference model. DUEL is the first metric sensitive to *both* components without reference model bias. Just as perplexity captures intrinsic quality for autoregressive models, DUEL perplexity provides the analogous metric for MDMs.

New Experiments. DUEL enables two categories of experiments:

- **Accurate MDM–AR comparison.** We can compare MDMs and AR models via perplexity under their respective test-time distributions, rather than the ELBO’s systematic underestimate (Section 6.1).
- **Reliable evaluation of sampling strategies.** We can isolate the effect of the unmasking policy by fixing the denoiser x_{θ} and varying the rule F , or conversely isolate the denoiser by fixing F and comparing different models (Section 6.2). The ELBO ignores the policy entirely, and generative perplexity conflates both components with reference model bias.

Limitations. Like ARM perplexity, DUEL ignores token sampling strategies (nucleus, top- k) used at generation time. Computationally, DUEL requires one forward pass per unmasking step—matching generation cost but exceeding the ELBO’s 1–128 Monte Carlo samples. Finally, downstream

Table 2. In-domain test perplexity (\downarrow) on OWT. ARM baseline: 17.54. **Bold**: best MDM. Gap closed defined in Equation (7).

Model	ELBO	DUEL	Gap Closed
SEDD	≤ 24.10	22.58	23.2%
MDLM	≤ 22.98	21.86	20.6%
BD3-LM $L'=4$	≤ 20.73	19.73	31.3%
BD3-LM $L'=8$	≤ 21.68	20.37	31.6%
BD3-LM $L'=16$	≤ 22.27	20.76	31.9%

Table 3. In-domain test perplexity (\downarrow) on LM1B. ARM baseline: 22.83. **Bold**: best MDM. Gap closed defined in Equation (7).

Model	ELBO	DUEL	Gap Closed
SEDD	≤ 32.68	31.51	11.9%
MDLM	≤ 31.78	29.03	30.7%
BD3-LM $L'=4$	≤ 28.23	26.97	23.3%
BD3-LM $L'=8$	≤ 29.83	27.85	28.3%
BD3-LM $L'=16$	≤ 30.60	28.39	28.4%

benchmarks remain useful for measuring capabilities perplexity does not capture.

6. Experiments

We demonstrate DUEL through two categories of experiments. First, we quantify how much of the perplexity gap between MDMs and ARMs is due to evaluation methodology (Section 6.1). Second, we use DUEL to compare sampling strategies—an analysis impossible with the ELBO and unreliable with generative perplexity (Section 6.2).

6.1. Perplexity Gap

Setup. MDMs have consistently lagged behind ARMs in perplexity benchmarks (Nie et al., 2024). We evaluate whether this gap is inflated by evaluation methodology. We compare an ARM baseline, SEDD (Lou et al., 2024), MDLM (Sahoo et al., 2024), and BD3-LM (Arriola et al., 2025a) with block sizes $L' \in \{4, 8, 16\}$, all trained with comparable model sizes, compute budgets, and data. All MDMs use greedy confidence unmasking restricted to a given block size. We evaluate *in-domain* on OpenWebText (OWT) and LM1B (Tables 2 and 3), *zero-shot* on PTB, Wikitext, LM1B, Lambada, and AG News (Table 4; full results in Table 8), and at *large scale* with LLaDA-8B (Nie et al., 2025) and Llama3-8B (Touvron et al., 2023) on Wikitext, Lambada, and AG News (Table 5). Details in Section D.1.

Metric. We define the *perplexity gap* $\Delta = \text{PPL}_{\text{MDM}} - \text{PPL}_{\text{ARM}}$. Since the ELBO yields an upper bound, Δ_{ELBO} may overestimate the true gap; DUEL gives exact perplexity. The *gap closed* measures what fraction of the ELBO gap is

Table 4. Gap closed (%) by DUEL on zero-shot evaluation (Equation (7)). Models trained on OWT; BD3-LM uses $L' = 4$. Full perplexity values in Table 8.

Dataset	SEDD	MDLM	BD3-LM
PTB	31.3%	34.3%	81.8%
Wikitext	40.8%	28.5%	31.4%
LM1B	22.1%	29.0%	29.8%
AG News	25.7%	27.8%	51.7%
Average	30.0%	29.9%	48.7%

Table 5. Zero-shot perplexity (\downarrow) for 8B models. **Bold**: better of ELBO/DUEL.

Model	Method	Wikitext	Lambada	AG News
Llama3	Exact	7.94	32.40	41.29
LLaDA	ELBO	≤ 15.29	≤ 39.04	≤ 85.17
	DUEL	14.50	36.00	78.91

eliminated by exact evaluation:

$$\text{Gap Closed (\%)} = \frac{\Delta_{\text{ELBO}} - \Delta_{\text{DUEL}}}{\Delta_{\text{ELBO}}} \times 100. \quad (7)$$

In-Domain Results. Tables 2 and 3 show test-set perplexity on OWT and LM1B. Across all models, DUEL closes 21–32% of the gap on OWT and 12–31% on LM1B.

Zero-Shot Results. Table 4 summarizes the gap closed on zero-shot benchmarks (full perplexities in Table 8). DUEL closes 30% of the gap on average, with BD3-LM reaching 82% on PTB.

Large-Scale Results. Table 5 scales to 8B parameters; DUEL consistently reduces LLaDA perplexity across all datasets, confirming exact evaluation applies at scale. Since LLaDA and Llama3 differ in training data and compute, we report only raw perplexity.

Takeaway. Proper perplexity evaluation via DUEL *substantially* closes the MDM–ARM perplexity gap. The gains come entirely from evaluation, not model changes: the ELBO averages over all orderings equally, including poor ones; DUEL evaluates under the deterministic policies that avoid such orderings.

6.2. Comparing Sampling Strategies

DUEL enables controlled comparison of unmasking rules (varying F , fixed x_θ) and denoisers (varying x_θ , fixed F) via exact likelihood. The ELBO cannot compare samplers—it ignores unmasking policy—while generative perplexity relies on biased reference models. We demonstrate through

Table 6. DUEL perplexity (\downarrow) by unmasking rule on OWT. Model: BD3-LM ($L'=16$). ELBO: ≤ 23.52 . **Bold**: best per NFE.

Unmask Rule F	128	256	512	1024
Left-to-Right	240.27	109.71	45.99	21.46
Greedy Conf.	164.94	66.64	34.74	22.03
Prob. Margin	140.38	57.48	32.24	22.05
Conf. Thresh. [†]	226.97	116.83	43.48	22.05

[†] Adaptive NFE; thresholds chosen to approximate target NFE.

Table 7. Oracle perplexity (\downarrow) on AG News for BD3-LM ($L' = 4$). All DUEL evaluations use block-restricted unmasking with $L' = 4$. The oracle searches all $4! = 24$ block permutations.

Model	Method	Unmask Rule F	Perplexity
ARM	Exact	—	52.11
BD3-LM	ELBO	—	≤ 61.67
BD3-LM	DUEL	Left-to-Right	54.94
	DUEL	Greedy Conf.	56.73
	DUEL	Prob. Margin	57.80
	DUEL	Conf. Thresh. [†]	55.68
BD3-LM	DUEL	Oracle	36.47

[†] Adaptive NFE; thresholds chosen to approximate target NFE.

two experiments: fast sampler comparison (Section 6.2.1) and optimal ordering exploration (Section 6.2.2).

6.2.1. COMPARING FAST SAMPLERS

MDMs generate by iteratively unmasking tokens over multiple steps, where the number of function evaluations (NFE) controls the trade-off between generation quality and speed. Fewer NFE enable greater parallelism—the key advantage of MDMs over ARMs—but risk degrading output quality. We compare four unmasking rules—left-to-right, greedy confidence, probability margin, and confidence threshold—across NFE budgets, and show that DUEL provides reliable rankings where generative perplexity fails.

Setup. We evaluate BD3-LM ($L' = 16$) trained on OWT. We vary $NFE \in \{128, 256, 512, 1024\}$ and report DUEL perplexity alongside generative perplexity (via GPT-2), entropy, and MAUVE computed from generated samples. The ELBO (≤ 23.52) is invariant to unmasking rules and NFE.

Results. Table 6 reports DUEL perplexity. At 1024 NFE, all rules converge to similar perplexity (≈ 21 – 22). At lower NFE, probability margin consistently achieves the lowest perplexity, followed closely by greedy confidence. At 128 NFE, probability margin (140.38) outperforms greedy confidence (164.94), the next-best rule.

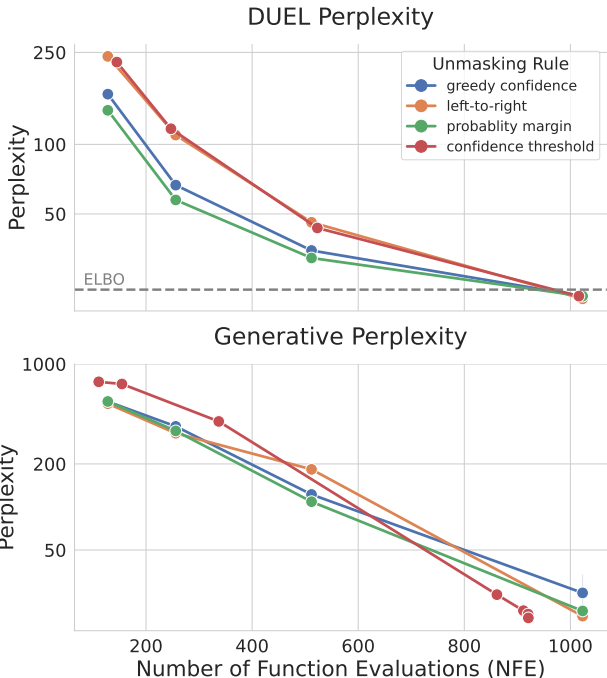


Figure 4. **Comparing fast samplers.** **Top:** DUEL perplexity. **Bottom:** Generative perplexity. Dashed line: ELBO (≤ 23.52). DUEL yields consistent rankings across NFE (probability margin best at low NFE, convergence at high NFE). Generative perplexity rankings cross repeatedly, making it unreliable.

DUEL Gives Consistent Rankings. Figure 4 (top) shows that DUEL perplexity yields *consistent* rankings across NFE budgets: probability margin is best at low NFE, followed by greedy confidence, with all methods converging at high NFE. This enables principled sampler selection—practitioners can confidently choose probability margin when compute is limited.

Generative Perplexity Fails at Low NFE. Figure 4 (bottom) reveals that generative perplexity rankings cross repeatedly. Strikingly, left-to-right achieves the *lowest* generative perplexity at 128 and 256 NFE despite having the *worst* DUEL perplexity. Entropy explains this discrepancy: left-to-right produces low-entropy degenerate text at low NFE, which autoregressive evaluators reward with low perplexity. Sample-based metrics also distort magnitude: generative perplexity shows 30–40 \times degradation at 128 vs. 1024 NFE, while DUEL shows 6–11 \times . Full entropy and MAUVE results in Section D.2.1 confirm this: MAUVE saturates near zero at low NFE, providing little discriminative signal.

Takeaway. For evaluating fast sampling strategies, DUEL is essential: it provides the consistent, interpretable rankings needed to identify which methods degrade gracefully under compute constraints.

6.2.2. ORACLE PERPLEXITY

Setup. Since different rules yield different likelihoods (Section 6.2.1), we ask: what is the lowest perplexity achievable over *all* orderings? This question is only meaningful with exact DUEL likelihood—the ELBO cannot distinguish orderings—making it uniquely enabled by DUEL. For block diffusion BD3-LM ($L' = 4$), we exhaustively search all $4! = 24$ permutations per block, selecting the one minimizing negative log-likelihood—the *oracle* perplexity. Details in Section D.2.2.

Results. Table 7 reports results on AG News (Zhang et al., 2015) (see Section D.2.2 for details). Among standard rules, all achieve perplexities between 54.94 (left-to-right) and 57.80 (probability margin), close to the ARM baseline of 52.11. The oracle, exhaustively searching all $4! = 24$ permutations per block, achieves 36.47—far surpassing the ARM and all standard rules.

Takeaway. Unmasking order is a powerful lever unique to MDMs: the same model achieves vastly different perplexities depending on the ordering, and the optimal per-block permutation far surpasses even the autoregressive baseline.

Since the oracle requires ground-truth tokens, developing strategies that approach its performance without such access is a promising direction; recent work on lookahead unmasking (Lee et al., 2025) takes initial steps, using search to select orderings at test time.

7. Conclusion

Summary. We introduced DUEL, a framework that gives MDMs a proper perplexity metric—the natural analogue of autoregressive perplexity—via *exact* likelihood computation under *deterministic* unmasking policies used at test time. Deterministic unmasking collapses the intractable marginalization to a single path, enabling this without training modifications or continuous-time assumptions. Empirically, proper evaluation via DUEL closes up to 32% of the perplexity gap on in-domain test sets and 82% on zero-shot evaluation, demonstrating that previous comparisons systematically underestimated MDM performance. DUEL also enables principled sampler comparison—reliable rankings of fast samplers across compute budgets—and reveals via oracle search that MDMs can surpass ARM baselines with optimal orderings.

Related Work. Several works explore likelihood and generation order in discrete diffusion. Peng et al. (2025a) derive an ELBO decomposing unmasking into a planner and denoiser; we compute exact likelihood without bounds. Peng et al. (2025b) extend this to joint training; we require no

training modifications. Wang et al. (2025c) learn context-dependent orderings via variational bounds; we evaluate exact likelihood under fixed deterministic policies. Jeon et al. (2025) establish the I-MDCE relation under optimal denoisers in continuous time; we operate in discrete time with trained networks. Our contribution is complementary: DUEL provides exact likelihood for existing pretrained MDMs without variational approximation, continuous-time assumptions, or architectural changes. See Section A for detailed related works.

Future Work. DUEL opens several directions: extending to remasking paradigms (Wang et al., 2025a; Huang et al., 2025) that allow iterative refinement; enabling GRPO-style reinforcement learning (Shao et al., 2024; Wang et al., 2025b) where importance ratios require exact probabilities; supporting speculative decoding (Guo & Ermon, 2025) that verifies parallel proposals via joint likelihoods; and applying to scientific domains (protein design, molecular generation) where likelihood-based evaluation is essential.

Impact Statement

This paper presents work whose goal is to advance the field of Machine Learning. There are many potential societal consequences of our work, none which we feel must be specifically highlighted here.

Acknowledgments

This work was partially funded by the National Science Foundation under award CAREER 2145577, and by the National Institute of Health under award MIRA R35GM151243. GT is partially supported by the NSF Graduate Research Fellowship under Grant No.DGE-213899. GT thanks Yair Schiff for insightful discussions and feedback.

References

- Arriola, M., Gokaslan, A., Chiu, J. T., Yang, Z., Qi, Z., Han, J., Sahoo, S. S., and Kuleshov, V. Block diffusion: Interpolating between autoregressive and diffusion language models. *arXiv preprint arXiv:2503.09573*, 2025a.
- Arriola, M., Schiff, Y., Phung, H., Gokaslan, A., and Kuleshov, V. Encoder-decoder diffusion language models for efficient training and inference. *arXiv preprint arXiv:2510.22852*, 2025b.
- Austin, J., Johnson, D. D., Ho, J., Tarlow, D., and Van Den Berg, R. Structured denoising diffusion models in discrete state-spaces. *Advances in neural information processing systems*, 34:17981–17993, 2021.

- Balloccu, S., Schmidtová, P., Lango, M., and Dušek, O. Leak, cheat, repeat: Data contamination and evaluation malpractices in closed-source llms. *arXiv preprint arXiv:2402.03927*, 2024.
- Ben-Hamu, H., Gat, I., Severo, D., Nolte, N., and Karrer, B. Accelerated sampling from masked diffusion models via entropy bounded unmasking. *arXiv preprint arXiv:2505.24857*, 2025.
- Bie, T., Cao, M., Chen, K., Du, L., Gong, M., Gong, Z., Gu, Y., Hu, J., Huang, Z., Lan, Z., et al. Llada2. 0: Scaling up diffusion language models to 100b. *arXiv preprint arXiv:2512.15745*, 2025.
- Campbell, A., Benton, J., De Bortoli, V., Rainforth, T., Deligiannidis, G., and Doucet, A. A continuous time framework for discrete denoising models. *Advances in Neural Information Processing Systems*, 35:28266–28279, 2022.
- Chang, H., Zhang, H., Jiang, L., Liu, C., and Freeman, W. T. Maskgit: Masked generative image transformer. In *Proceedings of the IEEE/CVF conference on computer vision and pattern recognition*, pp. 11315–11325, 2022.
- Chelba, C., Mikolov, T., Schuster, M., Ge, Q., Brants, T., Koehn, P., and Robinson, T. One billion word benchmark for measuring progress in statistical language modeling. *arXiv preprint arXiv:1312.3005*, 2013.
- Chen, Z., Fang, G., Ma, X., Yu, R., and Wang, X. dparallel: Learnable parallel decoding for dllms. *arXiv preprint arXiv:2509.26488*, 2025.
- Cohan, A., Dernoncourt, F., Kim, D. S., Bui, T., Kim, S., Chang, W., and Goharian, N. A discourse-aware attention model for abstractive summarization of long documents. *arXiv preprint arXiv:1804.05685*, 2018.
- Deschenaux, J. and Gulcehre, C. Beyond autoregression: Fast llms via self-distillation through time. *arXiv preprint arXiv:2410.21035*, 2024.
- Devlin, J., Chang, M.-W., Lee, K., and Toutanova, K. Bert: Pre-training of deep bidirectional transformers for language understanding. *arXiv preprint arXiv:1810.04805*, 2018.
- Devlin, J., Chang, M.-W., Lee, K., and Toutanova, K. Bert: Pre-training of deep bidirectional transformers for language understanding. In *Proceedings of the 2019 conference of the North American chapter of the association for computational linguistics: human language technologies, volume 1 (long and short papers)*, pp. 4171–4186, 2019.
- Dhariwal, P. and Nichol, A. Diffusion models beat gans on image synthesis. *Advances in neural information processing systems*, 34:8780–8794, 2021.
- Gat, I., Remez, T., Shaul, N., Kreuk, F., Chen, R. T., Synnaeve, G., Adi, Y., and Lipman, Y. Discrete flow matching. *Advances in Neural Information Processing Systems*, 37:133345–133385, 2024.
- Gokaslan, A., Cohen, V., Pavlick, E., and Tellex, S. Openwebtext corpus. <http://Skyllion007.github.io/OpenWebTextCorpus>, 2019.
- Gulrajani, I. and Hashimoto, T. B. Likelihood-based diffusion language models. *Advances in Neural Information Processing Systems*, 36, 2024.
- Guo, G. and Ermon, S. Reviving any-subset autoregressive models with principled parallel sampling and speculative decoding, 2025. URL <https://arxiv.org/abs/2504.20456>.
- Hayakawa, S., Takida, Y., Imaizumi, M., Wakaki, H., and Mitsufuji, Y. Distillation of discrete diffusion through dimensional correlations. *arXiv preprint arXiv:2410.08709*, 2024.
- Hayakawa, S., Takida, Y., Imaizumi, M., Wakaki, H., and Mitsufuji, Y. Demystifying maskgit sampler and beyond: Adaptive order selection in masked diffusion. *arXiv preprint arXiv:2510.04525*, 2025.
- Ho, J., Jain, A., and Abbeel, P. Denoising diffusion probabilistic models. *Advances in neural information processing systems*, 33:6840–6851, 2020.
- Hoogeboom, E., Gritsenko, A. A., Bastings, J., Poole, B., Berg, R. v. d., and Salimans, T. Autoregressive diffusion models. *arXiv preprint arXiv:2110.02037*, 2021a.
- Hoogeboom, E., Nielsen, D., Jaini, P., Forré, P., and Welling, M. Argmax flows and multinomial diffusion: Learning categorical distributions. *Advances in neural information processing systems*, 34:12454–12465, 2021b.
- Huang, Z., Wang, Y., Chen, Z., and Qi, G.-J. Don’t settle too early: Self-reflective remasking for diffusion language models. *arXiv preprint arXiv:2509.23653*, 2025.
- Jazbec, M., Olausson, T. X., Béthune, L., Ablin, P., Kirchhof, M., Monterio, J., Turrisi, V., Ramapuram, J., and Cuturi, M. Learning unmasking policies for diffusion language models. *arXiv preprint arXiv:2512.09106*, 2025.
- Jeon, M., Shin, S., Jeon, D., and No, A. Information-theoretic discrete diffusion. *arXiv preprint arXiv:2510.24088*, 2025.
- Kim, J., Shah, K., Kontonis, V., Kakade, S., and Chen, S. Train for the worst, plan for the best: Understanding token ordering in masked diffusions. *arXiv preprint arXiv:2502.06768*, 2025a.

- Kim, S. H., Hong, S., Jung, H., Park, Y., and Yun, S.-Y. Klass: Kl-guided fast inference in masked diffusion models. *arXiv preprint arXiv:2511.05664*, 2025b.
- Kingma, D., Salimans, T., Poole, B., and Ho, J. Variational diffusion models. *Advances in neural information processing systems*, 34:21696–21707, 2021.
- Kingma, D. P. and Welling, M. Auto-encoding variational bayes. *arXiv preprint arXiv:1312.6114*, 2013.
- Kuleshov, V. Fast algorithms for sparse principal component analysis based on rayleigh quotient iteration. In *International Conference on Machine Learning*, pp. 1418–1425. PMLR, 2013.
- Labs, I., Khanna, S., Kharbanda, S., Li, S., Varma, H., Wang, E., Birnbaum, S., Luo, Z., Miraoui, Y., Palrecha, A., et al. Mercury: Ultra-fast language models based on diffusion. *arXiv preprint arXiv:2506.17298*, 2025.
- Larochelle, H. and Murray, I. The neural autoregressive distribution estimator. In *Proceedings of the fourteenth international conference on artificial intelligence and statistics*, pp. 29–37. JMLR Workshop and Conference Proceedings, 2011.
- Lee, S., Kim, S., Park, J., and Park, D. Lookahead unmasking elicits accurate decoding in diffusion language models. *arXiv preprint arXiv:2511.05563*, 2025.
- Li, X., Thickstun, J., Gulrajani, I., Liang, P. S., and Hashimoto, T. B. Diffusion-lm improves controllable text generation. *Advances in Neural Information Processing Systems*, 35:4328–4343, 2022.
- Lou, A., Meng, C., and Ermon, S. Discrete diffusion modeling by estimating the ratios of the data distribution. In *Proceedings of the 41st International Conference on Machine Learning*, pp. 32819–32848, 2024.
- Luxembourg, O., Permuter, H., and Nachmani, E. Plan for speed-dilated scheduling for masked diffusion language models. *arXiv preprint arXiv:2506.19037*, 2025.
- Marcus, M., Santorini, B., and Marcinkiewicz, M. A. Building a large annotated corpus of english: The penn treebank. *Computational linguistics*, 19(2):313–330, 1993.
- Merity, S., Xiong, C., Bradbury, J., and Socher, R. Pointer sentinel mixture models. *arXiv preprint arXiv:1609.07843*, 2016.
- Nie, S., Zhu, F., Du, C., Pang, T., Liu, Q., Zeng, G., Lin, M., and Li, C. Scaling up masked diffusion models on text. *arXiv preprint arXiv:2410.18514*, 2024.
- Nie, S., Zhu, F., You, Z., Zhang, X., Ou, J., Hu, J., Zhou, J., Lin, Y., Wen, J.-R., and Li, C. Large language diffusion models. *arXiv preprint arXiv:2502.09992*, 2025.
- Ou, J., Nie, S., Xue, K., Zhu, F., Sun, J., Li, Z., and Li, C. Your absorbing discrete diffusion secretly models the conditional distributions of clean data. *arXiv preprint arXiv:2406.03736*, 2024.
- Paperno, D., Kruszewski, G., Lazaridou, A., Pham, N.-Q., Bernardi, R., Pezzelle, S., Baroni, M., Boleda, G., and Fernández, R. The lambada dataset: Word prediction requiring a broad discourse context. In *Proceedings of the 54th annual meeting of the association for computational linguistics (volume 1: Long papers)*, pp. 1525–1534, 2016.
- Peng, F. Z., Bezemek, Z., Patel, S., Rector-Brooks, J., Yao, S., Bose, A. J., Tong, A., and Chatterjee, P. Path planning for masked diffusion model sampling. *arXiv preprint arXiv:2502.03540*, 2025a.
- Peng, F. Z., Bezemek, Z., Rector-Brooks, J., Zhang, S., Zhang, A. R., Bronstein, M., Bose, A. J., and Tong, A. Planner aware path learning in diffusion language models training. *arXiv preprint arXiv:2509.23405*, 2025b.
- Pillutla, K., Swayamdipta, S., Zellers, R., Thickstun, J., Welleck, S., Choi, Y., and Harchaoui, Z. Mauve: Measuring the gap between neural text and human text using divergence frontiers. *Advances in Neural Information Processing Systems*, 34:4816–4828, 2021.
- Radford, A., Wu, J., Child, R., Luan, D., Amodei, D., Sutskever, I., et al. Language models are unsupervised multitask learners. *OpenAI blog*, 1(8):9, 2019.
- Sahoo, S., Arriola, M., Schiff, Y., Gokaslan, A., Marroquin, E., Chiu, J., Rush, A., and Kuleshov, V. Simple and effective masked diffusion language models. *Advances in Neural Information Processing Systems*, 37:130136–130184, 2024.
- Schiff, Y., Sahoo, S. S., Phung, H., Wang, G., Boshar, S., Dalla-torre, H., de Almeida, B. P., Rush, A., Pierrrot, T., and Kuleshov, V. Simple guidance mechanisms for discrete diffusion models. *arXiv preprint arXiv:2412.10193*, 2024.
- Shao, Z., Wang, P., Zhu, Q., Xu, R., Song, J., Bi, X., Zhang, H., Zhang, M., Li, Y., Wu, Y., et al. Deepseekmath: Pushing the limits of mathematical reasoning in open language models. *arXiv preprint arXiv:2402.03300*, 2024.
- Shi, J., Han, K., Wang, Z., Doucet, A., and Titsias, M. Simplified and generalized masked diffusion for discrete data. *Advances in neural information processing systems*, 37:103131–103167, 2024.

- Sohl-Dickstein, J., Weiss, E., Maheswaranathan, N., and Ganguli, S. Deep unsupervised learning using nonequilibrium thermodynamics. In *International conference on machine learning*, pp. 2256–2265. pmlr, 2015.
- Song, Y. and Ermon, S. Generative modeling by estimating gradients of the data distribution. *Advances in neural information processing systems*, 32, 2019.
- Song, Y., Sohl-Dickstein, J., Kingma, D. P., Kumar, A., Ermon, S., and Poole, B. Score-based generative modeling through stochastic differential equations. *arXiv preprint arXiv:2011.13456*, 2020.
- Song, Y., Zhang, Z., Luo, C., Gao, P., Xia, F., Luo, H., Li, Z., Yang, Y., Yu, H., Qu, X., et al. Seed diffusion: A large-scale diffusion language model with high-speed inference. *arXiv preprint arXiv:2508.02193*, 2025.
- Touvron, H., Lavril, T., Izacard, G., Martinet, X., Lachaux, M.-A., Lacroix, T., Rozière, B., Goyal, N., Hambro, E., Azhar, F., et al. Llama: Open and efficient foundation language models. *arXiv preprint arXiv:2302.13971*, 2023.
- Uria, B., Murray, I., and Larochelle, H. A deep and tractable density estimator. In *International Conference on Machine Learning*, pp. 467–475. PMLR, 2014.
- Uria, B., Côté, M.-A., Gregor, K., Murray, I., and Larochelle, H. Neural autoregressive distribution estimation. *Journal of Machine Learning Research*, 17(205): 1–37, 2016.
- Wang, G., Schiff, Y., Sahoo, S. S., and Kuleshov, V. Re-masking discrete diffusion models with inference-time scaling. *arXiv preprint arXiv:2503.00307*, 2025a.
- Wang, G., Schiff, Y., Turok, G., and Kuleshov, V. d2: Improved techniques for training reasoning diffusion language models. *arXiv preprint arXiv:2509.21474*, 2025b.
- Wang, P., Li, L., Chen, L., Cai, Z., Zhu, D., Lin, B., Cao, Y., Kong, L., Liu, Q., Liu, T., et al. Large language models are not fair evaluators. In *Proceedings of the 62nd Annual Meeting of the Association for Computational Linguistics (Volume 1: Long Papers)*, pp. 9440–9450, 2024.
- Wang, Y., Schiff, Y., Gokaslan, A., Pan, W., Wang, F., De Sa, C., and Kuleshov, V. InfoDiffusion: Representation learning using information maximizing diffusion models. In Krause, A., Brunskill, E., Cho, K., Engelhardt, B., Sabato, S., and Scarlett, J. (eds.), *Proceedings of the 40th International Conference on Machine Learning*, volume 202 of *Proceedings of Machine Learning Research*, pp. 36336–36354. PMLR, 23–29 Jul 2023. URL <https://proceedings.mlr.press/v202/wang23ah.html>.
- Wang, Z., Shi, J., Heess, N., Gretton, A., and Titsias, M. K. Learning-order autoregressive models with application to molecular graph generation. *arXiv preprint arXiv:2503.05979*, 2025c.
- White, C., Dooley, S., Roberts, M., Pal, A., Feuer, B., Jain, S., Shwartz-Ziv, R., Jain, N., Saifullah, K., Naidu, S., et al. Livebench: A challenging, contamination-free llm benchmark. *arXiv preprint arXiv:2406.19314*, 4, 2024.
- Wu, C., Zhang, H., Xue, S., Liu, Z., Diao, S., Zhu, L., Luo, P., Han, S., and Xie, E. Fast-dllm: Training-free acceleration of diffusion llm by enabling kv cache and parallel decoding. *arXiv preprint arXiv:2505.22618*, 2025.
- Yang, Z., Dai, Z., Yang, Y., Carbonell, J., Salakhutdinov, R. R., and Le, Q. V. Xlnet: Generalized autoregressive pretraining for language understanding. *Advances in neural information processing systems*, 32, 2019.
- Ye, J., Xie, Z., Zheng, L., Gao, J., Wu, Z., Jiang, X., Li, Z., and Kong, L. Dream 7b, 2025. URL <https://hkunlp.github.io/blog/2025/dream>.
- Zhang, X., Zhao, J., and LeCun, Y. Character-level convolutional networks for text classification. *Advances in neural information processing systems*, 28, 2015.
- Zheng, K., Chen, Y., Mao, H., Liu, M.-Y., Zhu, J., and Zhang, Q. Masked diffusion models are secretly time-agnostic masked models and exploit inaccurate categorical sampling. *arXiv preprint arXiv:2409.02908*, 2024.

A. Related Works

Masked Diffusion Models. Diffusion models were developed for continuous data (Sohl-Dickstein et al., 2015; Ho et al., 2020; Song et al., 2020) and extended to discrete state-spaces (Hoogeboom et al., 2021b; Austin et al., 2021; Campbell et al., 2022). Lou et al. (2024) proposed SEDD with a score-entropy objective. The absorbing (masking) kernel proved particularly effective, leading Sahoo et al. (2024) and Shi et al. (2024) to develop Masked Diffusion Models (MDM) with simplified training. Zheng et al. (2024) showed MDMs can be interpreted as time-agnostic masked models. MDMs have since scaled dramatically: Nie et al. (2025) introduced LLaDA at 8B parameters, Bie et al. (2025) scaled to 100B, and Labs et al. (2025); Song et al. (2025) demonstrated ultra-fast inference. Arriola et al. (2025a) proposed Block Diffusion interpolating between autoregressive and diffusion paradigms, and Arriola et al. (2025b) introduced E2D2, an encoder-decoder architecture enabling efficient training and KV caching.

Any-order Autoregressive Models. Standard autoregressive models generate left-to-right, but flexible generation orders benefit many tasks. NADE (Larochelle & Murray, 2011; Uria et al., 2016; 2014) pioneered order-agnostic density estimation. XLNet (Yang et al., 2019) proposed permutation language modeling. Hoogeboom et al. (2021a) connected autoregressive and diffusion models. Crucially, MDMs can be reinterpreted as any-order autoregressive models (AO-ARMs): Ou et al. (2024) established equivalence between absorbing diffusion objectives and AO-ARM likelihoods, while Zheng et al. (2024) interpreted MDMs as order-agnostic learners. Kim et al. (2025a) analyzed the exponentially larger masking space MDMs must handle compared to autoregressive models, showing that adaptive inference can mitigate training challenges. Wang et al. (2025c) introduced Learning-Order ARMs (LO-ARMs) that learn context-dependent orderings via a trainable order-policy, achieving state-of-the-art results on molecular graph generation.

Likelihood in Masked Diffusion. Several works derive variational bounds for MDMs: Sahoo et al. (2024) derived a Rao-Blackwellized ELBO as weighted masked language modeling losses, Shi et al. (2024) showed the continuous-time objective is a weighted cross-entropy integral, and Ou et al. (2024) connected these to AO-ARM likelihoods. Jeon et al. (2025) established that cross-entropy losses are tight likelihood estimators under optimal denoisers via the I-MDCE relation. However, their framework assumes continuous-time integral decompositions with optimal denoisers—conditions that differ from practical finite-step sampling with trained networks. Peng et al. (2025a) derived an ELBO that decomposes unmasking into a planner and denoiser, using an external planner to guide sampling; Peng et al. (2025b) extended this to training, jointly learning both components via the P-ELBO. Our work differs: rather than deriving bounds or modifying training, we show standard MDM training already enables exact likelihood evaluation under deterministic samplers.

Masked Diffusion Samplers. MDM sampling can be improved along two axes: the *unmasking policy* π (which positions to reveal) and the *denoiser* p_θ (which tokens to predict) with neural network x_θ . *Unmasking policy improvements.* Heuristic policies include random uniform sampling, confidence-based selection (Chang et al., 2022; Nie et al., 2025), entropy-based prioritization (Ben-Hamu et al., 2025), and margin-based methods (Kim et al., 2025a). KLASS (Kim et al., 2025b) adds a KL-stability criterion to filter confident-but-unstable predictions. Truly learned policies include Jazbec et al. (2025), who train a policy network to select positions. Scheduling methods (Luxembourg et al., 2025; Hayakawa et al., 2025) optimize the unmasking trajectory over time. *Denoiser improvements.* Methods improve x_θ through distillation (Deschenaux & Gulcehre, 2024; Hayakawa et al., 2024) or architectural changes enabling parallel decoding (Wu et al., 2025; Chen et al., 2025). *Remasking strategies.* Orthogonal to both axes, remasking (Wang et al., 2025a; Huang et al., 2025) allows reconsidering previous decisions by re-masking tokens, enabling iterative refinement absent in standard MDMs. Our framework applies to any deterministic unmasking policy where position selection is fixed given model predictions; extending to remasking is a direction for future work.

Evaluating Generative Models. Perplexity is the standard metric for language models, measuring predictive fit to held-out data, though it has known limitations: it ignores generation quality, can be gamed by degenerate distributions, and does not necessarily capture downstream capabilities. For MDMs, autoregressive perplexity cannot be directly computed; instead, the ELBO provides an upper bound on negative log-likelihood, which translates to a bound on perplexity. However, this bound can be loose and measures the wrong distribution (uniform position selection rather than test-time deterministic policies). When exact likelihood is unavailable, practitioners turn to *sample-based metrics*. Generative perplexity scores model samples under an external reference model (typically GPT-2), but inherits the reference model’s biases and ignores sample diversity—a model that repeats one high-quality phrase achieves excellent generative perplexity despite mode collapse. Post-hoc fixes like entropy (measuring diversity) and MAUVE (Pillutla et al., 2021) (comparing generated and reference

distributions) attempt to address these issues but remain imperfect: entropy is a secondary diagnostic without guidance on how to trade off against quality, while MAUVE inherits reference model bias and is hyperparameter-sensitive. *Benchmarks* (e.g., MMLU, GSM8K) measure task performance but suffer from data contamination (Balloccu et al., 2024) and gaming (White et al., 2024). Our DUEL exact likelihood computation resolves these issues: it provides a principled per-sample metric that evaluates the test-time distribution directly, requires only the MDM itself, and enables direct comparison with autoregressive models on the same probabilistic footing.

B. Extended Background

We present masked diffusion models (MDMs) and their interpretation as any-order autoregressive models (AO-ARMs). Section B.1 introduces the standard latent-variable formulation following Sahoo et al. (2024); Shi et al. (2024). Section B.2 recasts MDMs as AO-ARMs, making explicit the decomposition into position selection and token prediction—a perspective implicit in prior work but essential for our exact likelihood results.

B.1. Masked Diffusion Models

Forward Process. Let $\mathcal{V} = \{1, \dots, V\}$ denote a vocabulary of V tokens, augmented with a mask token $m \notin \mathcal{V}$ to form $\bar{\mathcal{V}} = \mathcal{V} \cup \{m\}$. A clean sequence is $\mathbf{x} = (x^{(1)}, \dots, x^{(L)}) \in \mathcal{V}^L$, and a partially masked sequence $\mathbf{z}_t \in \bar{\mathcal{V}}^L$ has some positions set to m . We write $\mathcal{M}(\mathbf{z}) = \{\ell : z_\ell = m\}$ for the set of masked positions.

The forward process progressively masks a clean sequence \mathbf{x} through T discrete steps. We index steps by $t \in \{0, 1, \dots, T\}$, corresponding to normalized time $t/T \in [0, 1]$. Let \mathbf{e}_v denote the one-hot vector for token v , and let $\alpha_t \in [0, 1]$ be a noise schedule with $\alpha_0 = 1$ (no corruption) and $\alpha_T = 0$ (fully masked). The forward transition from step s to t (where $0 \leq s < t \leq T$) factorizes independently across positions as $q_{t|s}(\mathbf{z}_t | \mathbf{z}_s) = \prod_{\ell=1}^L q_{t|s}(z_t^{(\ell)} | z_s^{(\ell)})$, where

$$q_{t|s}(z_t^{(\ell)} | z_s^{(\ell)}) = \text{Cat}(\alpha_{t|s} \mathbf{e}_{z_s^{(\ell)}} + (1 - \alpha_{t|s}) \mathbf{e}_m),$$

for $\alpha_{t|s} = \alpha_t / \alpha_s$. Each position independently either remains in its current state (with probability $\alpha_{t|s}$) or transitions to the mask token (with probability $1 - \alpha_{t|s}$). The mask token is an *absorbing state*: positions already masked remain masked. The forward marginal $q_{t|0}(\mathbf{z}_t | \mathbf{x})$ follows as a special case with $s = 0$ and $\mathbf{z}_0 = \mathbf{x}$:

$$q_{t|0}(z_t^{(\ell)} | x^{(\ell)}) = \text{Cat}(\alpha_t \mathbf{e}_{x^{(\ell)}} + (1 - \alpha_t) \mathbf{e}_m).$$

The complete forward trajectory distribution factorizes as:

$$q(\mathbf{z}_{0:T} | \mathbf{x}) = q(\mathbf{z}_0 | \mathbf{x}) \prod_{t=1}^T q_{t|t-1}(\mathbf{z}_t | \mathbf{z}_{t-1}), \quad (8)$$

where $q(\mathbf{z}_0 | \mathbf{x}) = \prod_{\ell=1}^L \text{Cat}(\mathbf{e}_{x^{(\ell)}})$ deterministically sets $\mathbf{z}_0 = \mathbf{x}$, then applies noising transitions $q_{t|t-1}$ that progressively mask tokens until step T .

Reverse Process. The reverse transition from step t to $s < t$ factorizes as $q_{s|t}(\mathbf{z}_s | \mathbf{z}_t, \mathbf{x}) = \prod_{\ell=1}^L q_{s|t}(z_s^{(\ell)} | \mathbf{z}_t, \mathbf{x})$, where

$$q_{s|t}(z_s^{(\ell)} | \mathbf{z}_t, \mathbf{x}) = \begin{cases} \text{Cat}(\mathbf{e}_{z_t^{(\ell)}}) & \text{if } z_t^{(\ell)} \neq m \\ \text{Cat}(\beta_{s|t} \mathbf{e}_m + \gamma_{s|t} \mathbf{e}_{x^{(\ell)}}) & \text{if } z_t^{(\ell)} = m \end{cases} \quad (9)$$

with $\beta_{s|t} = (1 - \alpha_s) / (1 - \alpha_t)$ and $\gamma_{s|t} = (\alpha_s - \alpha_t) / (1 - \alpha_t)$. Unmasked positions remain unchanged; masked positions either stay masked (with probability $\beta_{s|t}$) or reveal their true value (with probability $\gamma_{s|t}$).

Since \mathbf{x} is unknown at generation time, we learn a *denoising network* $x_\theta : \bar{\mathcal{V}}^L \rightarrow \mathbb{R}^{L \times V}$ that takes a partially masked sequence \mathbf{z} and outputs logits predicting clean tokens at each position. Following the SUBS parameterization (Sahoo et al., 2024), mask logits are set to $-\infty$ and unmasked positions copy their observed values. We define the token probability matrix $\mathbf{P} = \text{softmax}(x_\theta(\mathbf{z})) \in \Delta_V^L$ and the *denoising distribution* $p_\theta(v | \mathbf{z}) \triangleq P_\ell[v]$, the probability assigned to token v at position ℓ . The approximate reverse transition substitutes the denoising distribution for the unknown ground truth in Equation (9):

$$p_\theta(z_s^{(\ell)} | \mathbf{z}_t) = q_{s|t}(z_s^{(\ell)} | \mathbf{z}_t, \mathbf{x} \leftarrow \mathbf{P}).$$

The complete reverse trajectory distribution factorizes as:

$$p_\theta(\mathbf{x}, \mathbf{z}_{0:T}) = p(\mathbf{z}_T) \cdot p(\mathbf{x} | \mathbf{z}_0) \prod_{t=1}^T p_\theta(\mathbf{z}_{t-1} | \mathbf{z}_t),$$

where $p(\mathbf{z}_T) = \prod_{\ell=1}^L \text{Cat}(\mathbf{e}_m)$ is the fully masked prior, $p_\theta(\mathbf{z}_{t-1} | \mathbf{z}_t)$ are the learned denoising transitions applied backward to $t = 0$, and $p(\mathbf{x} | \mathbf{z}_0) = \prod_{\ell=1}^L \text{Cat}(\mathbf{e}_{z_0^{(\ell)}})$ deterministically emits $\mathbf{x} = \mathbf{z}_0$.

Likelihood and ELBO. The data likelihood marginalizes over latent trajectories: $p_\theta(\mathbf{x}) = \sum_{\mathbf{z}_{0:T}} p_\theta(\mathbf{x}, \mathbf{z}_{0:T})$. This sum is intractable, so we apply importance sampling with the forward process (8) as proposal and Jensen’s inequality:

$$\log p_\theta(\mathbf{x}) = \log \mathbb{E}_{q(\mathbf{z}_{0:T} | \mathbf{x})} \left[\frac{p_\theta(\mathbf{x}, \mathbf{z}_{0:T})}{q(\mathbf{z}_{0:T} | \mathbf{x})} \right] \geq \mathbb{E}_{q(\mathbf{z}_{0:T} | \mathbf{x})} \left[\log \frac{p_\theta(\mathbf{x}, \mathbf{z}_{0:T})}{q(\mathbf{z}_{0:T} | \mathbf{x})} \right].$$

Training Objective. Following Sahoo et al. (2024), the ELBO simplifies to a weighted sum of cross-entropy losses over masked positions in continuous time:

$$\mathcal{L}_{\text{ELBO}}(\theta) = \mathbb{E}_{\substack{t \sim \text{Unif}\{0,1\} \\ \mathbf{z}_t \sim q_{t|0}(\cdot | \mathbf{x})}} \left[w_t \sum_{\ell \in \mathcal{M}(\mathbf{z}_t)} -\log P_\ell[x^{(\ell)}] \right], \quad (10)$$

where $\mathbf{P} = \text{softmax}(x_\theta(\mathbf{z}_t))$ gives token probabilities at each position. The loss sums the negative log-probabilities $-\log P_\ell[x^{(\ell)}]$ of the true tokens $x^{(\ell)}$ at all masked positions $\ell \in \mathcal{M}(\mathbf{z}_t)$, weighted by $w_t = \alpha'_t / (1 - \alpha_t)$ with $\alpha'_t = d\alpha_t/dt$. In practice, MDMs use time-embedding-free architectures where x_θ depends only on \mathbf{z}_t , since the mask pattern implicitly encodes t .

B.2. Interpretation as Any-Order Autoregressive Models

We reformulate MDMs as any-order autoregressive models (AO-ARMs), which cleanly separates generation into two distinct operations: (1) an *unmasking policy* that selects which positions to reveal, and (2) a *denoising network* that predicts tokens at those positions. This decomposition is essential for our exact likelihood results. Prior work has established the equivalence between MDMs and AO-ARMs (Hoogeboom et al., 2021a; Zheng et al., 2024), with recent work explicitly proving that the MDM and AO-ARM training objectives (ELBOs) are equivalent (Ou et al., 2024; Kim et al., 2025a). However, to our knowledge, no prior work explicitly derives the AO-ARM generative model formulation from first principles. We provide this derivation below, with the joint factorization proved in Section C.1 and the ELBO formulation in Section C.3.

Ordered Partitions. An *ordered partition* $\sigma = (\sigma_1, \dots, \sigma_T)$ (Theorem 4.1) specifies how positions are revealed across T discrete steps, where each $\sigma_t \subseteq [L] = \{1, \dots, L\}$ is the set of positions unmasked at step t . The parts satisfy:

$$\bigcup_{t=1}^T \sigma_t = [L], \quad \sigma_t \cap \sigma_{t'} = \emptyset.$$

When each part contains exactly one position ($|\sigma_t| = 1$ for all t), we have $T = L$ steps and recover *sequential unmasking*; when parts contain multiple positions, we obtain *parallel unmasking* with $T < L$ steps. We write $\sigma_{<t} \triangleq \sigma_1 \cup \dots \cup \sigma_{t-1}$ for the set of positions revealed before step t , and $\mathbf{x}^{\sigma_{<t}} \triangleq \{x^{(\ell)}\}_{\ell \in \sigma_{<t}}$ for the clean tokens at those positions. The denoising network constructs its input by placing clean tokens at positions $\sigma_{<t}$ and mask tokens elsewhere, with position IDs.

Forward Process. In MDMs, positions are masked independently with probability $1 - \alpha_t$, which induces a uniform distribution over masking orders. To mirror this in the AO-ARM formulation, we define the forward process as sampling ordered partitions uniformly. For sequential unmasking ($|\sigma_t| = 1$ for all t , so $T = L$), this reduces to:

$$q(\sigma) = \frac{1}{L!}.$$

This ensures the AO-ARM training objective remains equivalent to the MDM objective.

Reverse Process. The reverse process generates a sequence through T discrete steps. At each step t , we (i) select which masked positions to reveal, and (ii) predict the tokens at those positions. This defines a joint distribution over sequences and ordered partitions (derived in Section C.1):

$$p_\theta(\mathbf{x}, \sigma) = \prod_{t=1}^T \underbrace{\pi_\theta(\sigma_t | \mathbf{x}^{\sigma < t})}_{\text{position selection}} \cdot \underbrace{p_\theta(\mathbf{x}^{\sigma_t} | \mathbf{x}^{\sigma < t})}_{\text{token prediction}},$$

where $\mathbf{x}^{\sigma_t} \triangleq \{x^{(\ell)}\}_{\ell \in \sigma_t}$. The *unmasking policy* $\pi_\theta(\sigma_t | \mathbf{x}^{\sigma < t})$ specifies a distribution over which masked positions to unmask at step t . The token prediction term factorizes under conditional independence (Theorem C.1) as $p_\theta(\mathbf{x}^{\sigma_t} | \mathbf{x}^{\sigma < t}) = \prod_{\ell \in \sigma_t} p_\theta(x^{(\ell)} | \mathbf{x}^{\sigma < t})$, where $p_\theta(x^{(\ell)} | \mathbf{x}^{\sigma < t})$ is the denoising distribution at position ℓ . Standard MDMs use uniform random selection:

$$\pi^{\text{unif}}(\sigma_t | \mathbf{z}) = \frac{1}{|\mathcal{M}(\mathbf{z})|},$$

where $|\mathcal{M}(\mathbf{z})|$ is the number of masked positions remaining. Alternative policies may use the denoiser’s predictions \mathbf{P} to inform position selection. Since \mathbf{P} is a deterministic function of the context $\mathbf{x}^{\sigma < t}$, such dependencies are implicit in the conditioning.

Likelihood and ELBO. The marginal likelihood sums over all ordered partitions: $p_\theta(\mathbf{x}) = \sum_\sigma p_\theta(\mathbf{x}, \sigma)$. This sum is intractable, analogous to the intractable integral over continuous latent trajectories in MDM. Applying importance sampling with a uniform proposal $q(\sigma)$ and Jensen’s inequality yields the ELBO:

$$\log p_\theta(\mathbf{x}) = \log \mathbb{E}_{q(\sigma)} \left[\frac{p_\theta(\mathbf{x}, \sigma)}{q(\sigma)} \right] \geq \mathbb{E}_{q(\sigma)} \left[\log \frac{p_\theta(\mathbf{x}, \sigma)}{q(\sigma)} \right].$$

Training Objective. Under a time-embedding-free denoising network with sequential unmasking ($|\sigma_t| = 1$), the MDM objective (10) is equivalent to the AO-ARM loss:

$$\mathcal{L}_{\text{ELBO}}(\theta) = \mathbb{E}_{q(\sigma)} \left[\sum_{t=1}^T \sum_{\ell \in \sigma_t} -\log p_\theta(x^{(\ell)} | \mathbf{x}^{\sigma < t}) \right],$$

This is the expected negative log-likelihood when tokens are predicted in uniformly random order, derived in Section C.3. The equivalence between MDM and AO-ARM loss functions follows most directly from Kim et al. (2025a).

C. Proofs

C.1. Joint Factorization of the Reverse Process

We present the joint factorization directly for ordered partitions; the sequential case (one position per step) is a special case. The factorization relies on the following assumption about parallel token prediction.

Assumption C.1 (Conditional Independence Within Groups). Given the revealed tokens $\mathbf{x}^{\sigma < t}$, the tokens at positions within σ_t are predicted independently by the denoising network:

$$p_\theta(\mathbf{x}^{\sigma_t} | \mathbf{x}^{\sigma < t}) = \prod_{\ell \in \sigma_t} p_\theta(x^{(\ell)} | \mathbf{x}^{\sigma < t}),$$

where $p_\theta(x^{(\ell)} | \mathbf{x}^{\sigma < t}) \triangleq P_\ell[x^{(\ell)}]$ is the denoising distribution at position ℓ . The denoising network constructs its input by placing the clean tokens $\mathbf{x}^{\sigma < t}$ at their respective positions with mask tokens elsewhere, and outputs token probabilities $\mathbf{P} = \text{softmax}(x_\theta(\cdot))$.

This assumption is standard in MDM generation and holds by construction: the denoising network outputs independent distributions over tokens at each position. The assumption becomes an approximation when multiple tokens are sampled simultaneously, since the true joint distribution over tokens may have dependencies not captured by the factorized model. When each group contains exactly one position ($|\sigma_t| = 1$ for all t), we have $T = L$ steps and the ordered partition reduces to a permutation over positions; in this case, the assumption is trivially satisfied since each group contains a single token.

Proposition C.2 (Joint Factorization). *Let $\sigma = (\sigma_1, \dots, \sigma_T)$ be an ordered partition (Theorem 4.1), where $\sigma_t \subseteq [L]$ is the set of positions unmasked at step t . The joint distribution of sequence \mathbf{x} and ordered partition σ under the reverse process factorizes as:*

$$p_\theta(\mathbf{x}, \sigma) = \prod_{t=1}^T \pi_\theta(\sigma_t \mid \mathbf{x}^{\sigma_{<t}}) \cdot p_\theta(\mathbf{x}^{\sigma_t} \mid \mathbf{x}^{\sigma_{<t}}), \quad (11)$$

where $\sigma_{<t} \triangleq \sigma_1 \cup \dots \cup \sigma_{t-1}$, $\mathbf{x}^{\sigma_{<t}} \triangleq \{x^{(\ell)}\}_{\ell \in \sigma_{<t}}$ is the set of clean tokens at positions revealed before step t , and $\mathbf{x}^{\sigma_t} \triangleq \{x^{(\ell)}\}_{\ell \in \sigma_t}$. Under Theorem C.1, $p_\theta(\mathbf{x}^{\sigma_t} \mid \mathbf{x}^{\sigma_{<t}}) = \prod_{\ell \in \sigma_t} p_\theta(x^{(\ell)} \mid \mathbf{x}^{\sigma_{<t}})$.

Proof. Applying the chain rule, then factoring each term into position selection and token prediction:

$$\begin{aligned} p_\theta(\mathbf{x}, \sigma) &= \prod_{t=1}^T p_\theta(\mathbf{x}^{\sigma_t}, \sigma_t \mid \mathbf{x}^{\sigma_{<t}}, \sigma_{<t}) \\ &= \prod_{t=1}^T \pi_\theta(\sigma_t \mid \mathbf{x}^{\sigma_{<t}}, \sigma_{<t}) \cdot p_\theta(\mathbf{x}^{\sigma_t} \mid \sigma_t, \mathbf{x}^{\sigma_{<t}}, \sigma_{<t}) \\ &= \prod_{t=1}^T \pi_\theta(\sigma_t \mid \mathbf{x}^{\sigma_{<t}}) \cdot p_\theta(\mathbf{x}^{\sigma_t} \mid \mathbf{x}^{\sigma_{<t}}). \end{aligned}$$

The first equality is the chain rule; at $t = 1$, $p_\theta(\mathbf{x}^{\sigma_1}, \sigma_1 \mid \mathbf{x}^{\sigma_{<1}}, \sigma_{<1}) = p_\theta(\mathbf{x}^{\sigma_1}, \sigma_1)$ since $\mathbf{x}^{\sigma_{<1}} = \emptyset$ and $\sigma_{<1} = \emptyset$. The second factors each term via $p(A, B \mid C) = p(B \mid C) \cdot p(A \mid B, C)$. The third drops $\sigma_{<t}$ (redundant since $\mathbf{x}^{\sigma_{<t}}$ encodes positions via position indices) and drops σ_t from the denoiser (which predicts all masked positions simultaneously without σ_t as input). Applying Theorem C.1 yields Equation (11). \square

C.2. Proposal Distribution

For sequential unmasking ($|\sigma_t| = 1$ for all t), the forward masking process induces a uniform distribution over unmasking orders.

Proposition C.3 (Uniform Proposal Distribution). *Under sequential unmasking, the forward masking process induces a uniform distribution over unmasking orders:*

$$q(\sigma) = \frac{1}{L!} \quad \text{for all permutations } \sigma.$$

Proof. We relate the forward *masking* process to the reverse *unmasking* order.

Step 1: Forward masking process. Starting from $\mathbf{z}^{(0)} = \mathbf{x}$, at each step $t = 1, \dots, L$, we select one of the $L - t + 1$ currently unmasked positions uniformly at random and mask it. Let τ_t denote the position masked at step t . The probability of any specific masking order $\tau = (\tau_1, \dots, \tau_L)$ is:

$$q(\tau) = \prod_{t=1}^L \frac{1}{L - t + 1} = \frac{1}{L} \cdot \frac{1}{L-1} \cdots \frac{1}{1} = \frac{1}{L!}.$$

Step 2: Unmasking order reverses masking order. The unmasking order σ specifies the sequence in which positions are *revealed* during generation. This is the reverse of the masking order: position τ_L (last to be masked) is the first to be unmasked.

Step 3: Uniformity is preserved under reversal. Since reversal is a bijection on permutations, and $q(\tau) = 1/L!$ for all τ , we have $q(\sigma) = 1/L!$ for all σ . \square

C.3. Deriving the AO-ARM Training Objective (ELBO)

Although the ELBO training objective for MDMs has been established in prior work (Hoogeboom et al., 2021a; Ou et al., 2024; Kim et al., 2025a), we provide the derivation from first principles here for completeness. We derive the result for

sequential unmasking (one position per step), where σ is a permutation of $[L]$ and $\sigma_t \in [L]$ denotes the single position unmasked at step t . Sequential unmasking is required for the uniform proposal $q(\sigma) = 1/L!$ from Theorem C.3, which enables the policy–proposal cancellation in Step 2 of the proof.

Proposition C.4 (ELBO Training Objective). *Let $p_\theta(\mathbf{x}, \sigma)$ be the joint distribution from Theorem C.2 under sequential unmasking with uniform policy, and let $q(\sigma) = 1/L!$ be the proposal from Theorem C.3. Then:*

$$\log p_\theta(\mathbf{x}) \geq -\mathcal{L}_{ELBO}(\theta; \mathbf{x}),$$

where

$$\mathcal{L}_{ELBO}(\theta; \mathbf{x}) = \mathbb{E}_{q(\sigma)} \left[\sum_{t=1}^L -\log p_\theta(x^{(\sigma_t)} \mid \mathbf{x}^{\sigma_{<t}}) \right], \quad (12)$$

where $\sigma_t \in [L]$ is the position unmasked at step t .

Proof. We proceed in two steps.

Step 1: Importance sampling and Jensen’s inequality. The marginal likelihood requires summing over all $L!$ unmasking orders. We rewrite this as an expectation under the uniform proposal $q(\sigma) = 1/L!$:

$$p_\theta(\mathbf{x}) = \sum_{\sigma} p_\theta(\mathbf{x}, \sigma) = \sum_{\sigma} q(\sigma) \cdot \frac{p_\theta(\mathbf{x}, \sigma)}{q(\sigma)} = \mathbb{E}_{\sigma \sim q} \left[\frac{p_\theta(\mathbf{x}, \sigma)}{q(\sigma)} \right].$$

Taking logarithms and applying Jensen’s inequality:

$$\log p_\theta(\mathbf{x}) = \log \mathbb{E}_{\sigma \sim q} \left[\frac{p_\theta(\mathbf{x}, \sigma)}{q(\sigma)} \right] \geq \mathbb{E}_{\sigma \sim q} \left[\log \frac{p_\theta(\mathbf{x}, \sigma)}{q(\sigma)} \right] \triangleq -\mathcal{L}_{ELBO}(\theta; \mathbf{x}).$$

Step 2: Substituting factorizations and simplifying. From Theorems C.2 and C.3, we expand the log-ratio. With a uniform unmasking policy $\pi^{\text{unif}}(\sigma_t \mid \mathbf{x}^{\sigma_{<t}}) = 1/(L-t+1)$ (where $L-t+1$ is the number of remaining masked positions), the policy terms cancel with the proposal:

$$\log \frac{p_\theta(\mathbf{x}, \sigma)}{q(\sigma)} = \sum_{t=1}^L \underbrace{\log \frac{1/(L-t+1)}{1/(L-t+1)}}_{=0} + \sum_{t=1}^L \log p_\theta(x^{(\sigma_t)} \mid \mathbf{x}^{\sigma_{<t}}).$$

The first sum vanishes, yielding equation (12). □

C.4. Theoretical Properties of DUEL

We prove the main theoretical results for DUEL samplers: policy-dependent distributions and exact likelihood computation.

Definition C.5 (Order Sensitivity). A denoising network x_θ is *order-sensitive* if the predicted distribution at some masked position depends on which other tokens have been revealed. Formally, there exist positions $i \neq j$, a token v , and partial sequences \mathbf{z}, \mathbf{z}' where: (i) position j is masked in both, (ii) \mathbf{z} has token a revealed at position i while \mathbf{z}' has position i masked, and (iii) $p_\theta(v \mid j, \mathbf{z}) \neq p_\theta(v \mid j, \mathbf{z}')$.

In practice, trained MDMs are very likely to be order-sensitive: the network learns to condition predictions on revealed context to capture inter-position dependencies. We verify this empirically in our experiments (Section 6), where different unmasking rules yield different likelihoods. An order-insensitive network—one where predictions depend only on position—could not model token correlations.

Theorem C.6 (Policy-Dependent Distribution). *If x_θ is order-sensitive, there exist unmasking rules F_1, F_2 inducing different distributions: $p_\theta^{\pi^{F_1}} \neq p_\theta^{\pi^{F_2}}$.*

Proof of Theorem 4.2. By order-sensitivity, there exist positions $i \neq j$, token v , and partial sequences \mathbf{z}, \mathbf{z}' such that: position j is masked in both; \mathbf{z} has token a at position i while \mathbf{z}' has i masked; and $p_\theta(v \mid j, \mathbf{z}) \neq p_\theta(v \mid j, \mathbf{z}')$. Define F_1 to unmask i before j , and F_2 to unmask j before i . For the sequence \mathbf{x} with $x^{(i)} = a$ and $x^{(j)} = v$:

- Under F_1 : position j is predicted after i is revealed, contributing $\log p_\theta(v | j, \mathbf{z})$.
- Under F_2 : position j is predicted while i is masked, contributing $\log p_\theta(v | j, \mathbf{z}')$.

Since these terms differ, $p_\theta^{\pi^{F_1}}(\mathbf{x}) \neq p_\theta^{\pi^{F_2}}(\mathbf{x})$. \square

Remark C.7 (Order-Insensitive Networks). For completeness: if x_θ were order-insensitive, all policies would induce the same distribution, since $\log p_\theta^{\pi^F}(\mathbf{x}) = \sum_{\ell=1}^L \log p_\theta(x^{(\ell)} | \ell)$ would be independent of the trajectory.

Theorem C.8 (DUEL Exact Likelihood). *Under a deterministic policy π_θ^F , exactly one ordered partition $\sigma^* = (\sigma_1^*, \dots, \sigma_T^*)$ satisfies $p_\theta^{\pi^F}(\mathbf{x}, \sigma^*) > 0$. The log-likelihood is:*

$$\log p_\theta^{\pi^F}(\mathbf{x}) = \sum_{t=1}^T \sum_{\ell \in \sigma_t^*} \log p_\theta(x^{(\ell)} | \mathbf{x}^{\sigma_{<t}^*}), \quad (6)$$

where $\sigma_t^* = F(\mathbf{x}^{\sigma_{<t}^*})$ is the set of positions selected at step t .

Proof of Theorem 4.3. The key insight is that a deterministic policy eliminates the intractable sum over orderings: exactly one ordering has nonzero probability, so the sum collapses to a single computable term.

Step 1: The deterministic rule induces a unique trajectory. Given any sequence \mathbf{x} and a deterministic rule F , there is exactly one unmasking trajectory $\sigma^* = (\sigma_1^*, \dots, \sigma_T^*)$ that the generative process can follow. To see this, note that generation starts from the same fully masked state and proceeds deterministically: at step t , the rule F examines the current revealed tokens $\mathbf{x}^{\sigma_{<t}^*}$ and returns a fixed set of positions $\sigma_t^* = F(\mathbf{x}^{\sigma_{<t}^*})$. We then reveal the true tokens at those positions, yielding the next set of revealed tokens. Since F is a function (not a distribution) and revealed tokens remain fixed (the absorbing property), each step is uniquely determined by the previous state.

Step 2: All other orderings have zero probability. Consider any ordering $\sigma \neq \sigma^*$. Since σ differs from σ^* , there must be some first step t where $\sigma_t \neq \sigma_t^*$. At this step, the revealed tokens are identical (both orderings have revealed the same positions up to step $t-1$), so the rule returns the same positions: $F(\mathbf{x}^{\sigma_{<t}}) = F(\mathbf{x}^{\sigma_{<t}^*}) = \sigma_t^*$. But since $\sigma_t \neq \sigma_t^*$, we have $\sigma_t \neq F(\mathbf{x}^{\sigma_{<t}})$. By the definition of the deterministic policy (Equation (3)), $\pi_\theta^F(\sigma_t | \mathbf{x}^{\sigma_{<t}}) = 0$, which makes the entire joint probability $p_\theta^{\pi^F}(\mathbf{x}, \sigma) = 0$.

Step 3: The marginal reduces to a single term. Since all orderings except σ^* contribute zero probability, the marginal likelihood simplifies:

$$p_\theta^{\pi^F}(\mathbf{x}) = \sum_{\sigma} p_\theta^{\pi^F}(\mathbf{x}, \sigma) = p_\theta^{\pi^F}(\mathbf{x}, \sigma^*).$$

Expanding the surviving term using the joint factorization (Equation (2)):

$$p_\theta^{\pi^F}(\mathbf{x}, \sigma^*) = \prod_{t=1}^T \underbrace{\pi_\theta^F(\sigma_t^* | \mathbf{x}^{\sigma_{<t}^*})}_{=1} \cdot \prod_{\ell \in \sigma_t^*} p_\theta(x^{(\ell)} | \mathbf{x}^{\sigma_{<t}^*}).$$

Each policy term equals 1 because $\sigma_t^* = F(\mathbf{x}^{\sigma_{<t}^*})$ by construction. Taking logarithms yields Equation (6). \square

D. Experimental Details

We provide details for each experiment. Training and architecture follow Sahoo et al. (2024) and Arriola et al. (2025a).

D.1. Perplexity Gap Experiments

Data. We evaluate on two in-domain datasets: OpenWebText (OWT; Gokaslan et al., 2019) with GPT-2 tokenizer (Radford et al., 2019), and One Billion Words (LM1B; Chelba et al., 2013) with BERT tokenizer (Devlin et al., 2019). For zero-shot evaluation, we train on OWT and evaluate on Penn Tree Bank (Marcus et al., 1993), Wikitext (Merity et al., 2016), LM1B, Lambada (Paperno et al., 2016), AG News (Zhang et al., 2015), and Scientific Papers (PubMed and ArXiv subsets) (Cohan et al., 2018). All sequences are concatenated and wrapped following Arriola et al. (2025a). We use the full validation/test split for all evaluations. For large-scale experiments, we evaluate on Wikitext, Lambada, and AG News.

Models. For test and zero-shot perplexity, we evaluate: (1) an autoregressive model (ARM) baseline, (2) SEDD (Lou et al., 2024), (3) MDLM (Sahoo et al., 2024), and (4) BD3-LM (Arriola et al., 2025a) with block sizes $L' \in \{4, 8, 16\}$. All 110M models use 12-layer DiT, hidden dim 768, 12 heads, with sequence length $L = 1024$ (OWT) or $L = 128$ (LM1B), trained for 1M steps on 524B tokens with batch size 512, making them directly comparable. For large-scale experiments, we evaluate LLaDA-8B-Base (Nie et al., 2025) with sequence length $L = 2048$ and include Llama3-8B-Base (Touvron et al., 2023) as a reference; note these models differ in training data and compute budget, so we do not compute gap closed for this comparison.

Likelihood Estimators. We compare three methods for computing negative log-likelihood, listed as “Method” in our tables.

- **Exact** (ARM baseline). The autoregressive model computes exact log-likelihood via the chain rule of probability:

$$\log p(\mathbf{x}) = \sum_{\ell=1}^L \log p(x^{(\ell)} \mid x^{(1)}, \dots, x^{(\ell-1)}).$$

Each conditional is computed in a single, batched forward pass using causal masking, so the full log-likelihood requires one forward pass over the sequence.

- **ELBO** (MDMs). The ELBO provides an upper bound on the true negative log-likelihood. Because the MDM loss (Equation (1)) involves an expectation over random timesteps and masked positions, computing it exactly is intractable; instead, we use a K -sample Monte Carlo estimate of the ELBO. For MDLM/SEDD, the loss weights each masked position by L/n_t where n_t is the number of masked positions; for BD3-LM, the loss factorizes over blocks with preceding blocks revealed (see Arriola et al., 2025a, Eq. 8). We use $K = 1$ Monte Carlo sample with a low-discrepancy sampler (Kingma et al., 2021) for the 110M models, and $K = 128$ samples for LLaDA-8B.
- **DUEL** (MDMs). Computes exact likelihood under a deterministic unmasking policy by summing the log-probabilities of revealed tokens along the single path induced by the unmasking rule (Algorithm 1 in the main paper).

Metrics. Each likelihood estimator above produces a negative log-likelihood $NLL = -\log p(\mathbf{x})$ for a sequence \mathbf{x} of length L . We convert this to perplexity: $PPL = \exp(NLL/L)$. To compare MDMs against the ARM baseline, we define the *perplexity gap* $\Delta = PPL_{MDM} - PPL_{ARM}$. Under the ELBO, $\Delta_{ELBO} = PPL_{MDM}^{ELBO} - PPL_{ARM}$; under DUEL, $\Delta_{DUEL} = PPL_{MDM}^{DUEL} - PPL_{ARM}$. The *gap closed (%)* measures the fraction of the ELBO gap eliminated by exact evaluation:

$$\text{Gap Closed} = \frac{\Delta_{ELBO} - \Delta_{DUEL}}{\Delta_{ELBO}} \times 100\%.$$

Note that in zero-shot experiments (Table 4) we exclude Lambada, PubMed, and ArXiv datasets and do not report the gap closed metric. This is because the MDM already outperforms the ARM baseline under the ELBO on these datasets, making $\Delta_{ELBO} \leq 0$ and gap closed ill-defined; nonetheless, DUEL still yields similar-magnitude perplexity reductions on these datasets (Table 8).

Protocol. We evaluate on the full validation/test split for both ELBO and DUEL. For the 110M models, DUEL uses block-greedy unmasking with $k = 1$ token per step, restricted to block size $L' = 4$. For LLaDA-8B-Base, DUEL uses block-greedy unmasking with $k = 1$, restricted to block size $L' = 32$.

DUEL perplexity outperforms ELBO perplexity on every model and dataset comparison except one. The sole exception is MDLM on Lambada, where the ELBO (≤ 48.29) is slightly lower than DUEL (48.42); this is not contradictory, as they measure different distributions (p_{θ}^{unif} vs. $p_{\theta}^{\pi^F}$).

D.2. Comparing Sampling Strategies

This section provides experimental details for Section 6.2.

D.2.1. COMPARING FAST SAMPLERS

Data. OpenWebText (Gokaslan et al., 2019) validation split (1,000 samples, $L = 1024$, GPT-2 tokenizer).

Table 8. Zero-shot perplexity (\downarrow) for models trained on OWT, evaluated on unseen datasets. ARM baseline in first row. **Bold**: better of ELBO/DUEL per model-dataset pair.

Model	Method	PTB	Wikitext	LM1B	Lambada	AG News	PubMed	ArXiv
ARM	Exact	81.07	25.32	51.14	52.13	52.11	48.59	41.22
SEDD	ELBO	≤ 96.33	≤ 35.98	≤ 68.14	≤ 48.93	≤ 67.82	≤ 43.13	≤ 37.89
	DUEL	91.56	31.63	64.39	46.01	63.78	39.31	35.48
MDLM	ELBO	≤ 90.96	≤ 33.22	≤ 64.94	≤ 48.29	≤ 62.78	≤ 43.13	≤ 37.89
	DUEL	87.57	30.97	60.94	48.42	59.81	41.96	37.57
BD3-LM $L'=4$	ELBO	≤ 96.81	≤ 31.31	≤ 60.88	≤ 50.03	≤ 61.67	≤ 42.52	≤ 39.20
	DUEL	83.94	29.43	57.98	48.56	56.73	41.41	38.11

Model. BD3-LM (Arriola et al., 2025a) with block size $L' = 16$, trained on OWT.

Unmasking Rules. We compare four deterministic rules, all restricted to operate within blocks of size $L' = 16$:

1. **Left-to-Right:** $F(\mathbf{z}) = \{\min\{\ell : z_\ell = \mathbf{m}\}\}$
2. **Greedy Confidence:** $F(\mathbf{z}) = \arg \max_{\ell: z_\ell = \mathbf{m}} \max_v p_\theta(v | \mathbf{z})$
3. **Probability Margin (Kim et al., 2025a):** $F(\mathbf{z}) = \arg \max_{\ell: z_\ell = \mathbf{m}} \left(p_\theta^{(1)}(\ell | \mathbf{z}) - p_\theta^{(2)}(\ell | \mathbf{z}) \right)$, where $p_\theta^{(1)}, p_\theta^{(2)}$ are the top-2 token probabilities
4. **Confidence Threshold (Wu et al., 2025):** Unmask all ℓ where $\max_v p_\theta(v | \mathbf{z}) > \tau$; if none exceed τ , unmask the most confident position

Metrics. We report four metrics:

1. **DUEL perplexity (\downarrow):** Exact likelihood computed on OWT validation data
2. **Generative perplexity (\downarrow):** Generate 1,000 samples, evaluate under GPT-2 Large (Radford et al., 2019)
3. **Entropy (\uparrow):** Token-level entropy of generated text; low entropy indicates repetitive or degenerate output
4. **MAUVE (\uparrow) (Pillutla et al., 2021):** Distribution similarity between 1,000 generated samples and 1,000 reference sequences from OWT

Protocol. We vary the number of function evaluations (NFE) $\in \{128, 256, 512, 1024\}$ by adjusting the number of tokens unmasked per forward pass, $k \in \{8, 4, 2, 1\}$ respectively, for a sequence length of $L = 1024$. For left-to-right, greedy, and probability margin, k is fixed and the NFE is exactly $\lceil L/k \rceil$.

Confidence threshold adaptively selects how many tokens to unmask based on whether predictions exceed a threshold τ , so the NFE varies per sequence and differs between evaluation (on held-out data) and generation. For DUEL perplexity, we set $\tau \in \{0.05, 0.075, 0.15, 0.99\}$, yielding approximately $\{145, 259, 523, 1016\}$ NFE respectively. For sample generation (generative perplexity, entropy, MAUVE), the same thresholds yield approximately $\{138, 184, 493, 973\}$ NFE. Table 6 reports confidence threshold at the closest NFE to each target; Figure 5 plots all available data points.

Results. Figure 5 presents the full comparison across all four metrics.

DUEL perplexity. Rankings are consistent across NFE budgets: probability margin achieves the lowest perplexity at low NFE, followed by greedy confidence, with left-to-right and confidence threshold performing worst. All methods converge to similar perplexity (≈ 21 – 22) at 1024 NFE, approaching the ELBO baseline (≤ 23.52). The degradation from 1024 to 128 NFE ranges from $6\times$ (probability margin) to $11\times$ (left-to-right).

Generative perplexity. Rankings are inconsistent: left-to-right achieves the *lowest* generative perplexity at 128 and 256 NFE despite having the *worst* DUEL perplexity. This apparent contradiction is explained by the entropy results below. The magnitude of degradation is also distorted, showing 30 – $40\times$ increase from 1024 to 128 NFE.

DUEL: Exact Likelihood for Masked Diffusion via Deterministic Unmasking

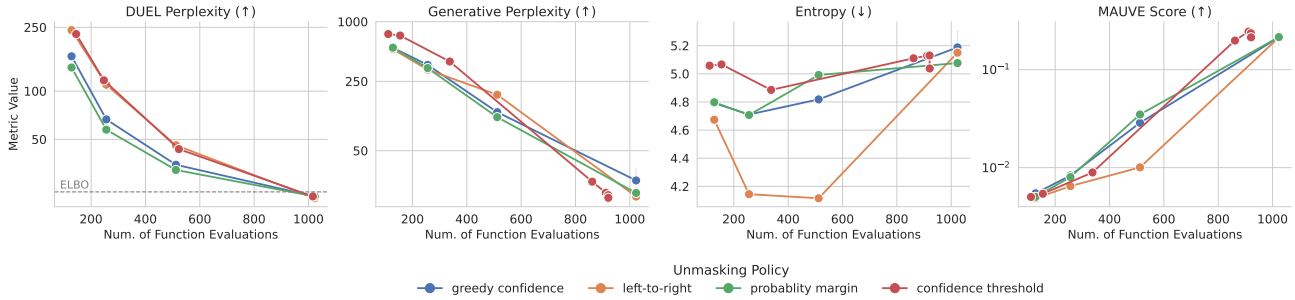


Figure 5. Comparing fast samplers across four metrics. Dashed line in DUEL perplexity: ELBO (≤ 23.52). DUEL perplexity yields consistent rankings across NFE (probability margin best at low NFE), while generative perplexity rankings cross repeatedly. Entropy reveals that left-to-right produces degenerate low-entropy text at low NFE despite achieving favorable generative perplexity. MAUVE saturates near zero at low NFE for all rules, providing little discriminative signal.

Entropy. Left-to-right exhibits anomalously low entropy (≈ 4.2) at low NFE, indicating degenerate, repetitive text. This explains its misleadingly favorable generative perplexity: repetitive text often achieves low perplexity under autoregressive models. In contrast, probability margin and greedy confidence maintain higher entropy (≈ 4.8 – 5.0) even at low NFE, indicating more diverse output. All methods converge to entropy ≈ 5.1 at 1024 NFE.

MAUVE. All methods achieve MAUVE < 0.02 at 128 NFE, providing minimal discriminative signal. Scores improve to 0.1 – 0.2 at 1024 NFE, but remain below typical thresholds for high-quality generation. The log-scale behavior indicates MAUVE is most useful for distinguishing high-quality regimes, not for comparing degraded generation.

Takeaways. Sample-based metrics can be misleading: generative perplexity rewards degenerate text, entropy requires careful interpretation, and MAUVE saturates at low quality. DUEL perplexity provides consistent, interpretable rankings that correctly identify probability margin as optimal at low NFE budgets.

D.2.2. ORACLE PERPLEXITY

Data. AG News (Zhang et al., 2015) zero-shot evaluation (GPT-2 tokenizer, $L = 1024$).

Model. BD3-LM with block size $L' = 4$, trained on OWT (same model as Section 6.1).

Method. For BD3-LM, DUEL processes each block of size L' independently. Within a block, the unmasking order is a permutation $\pi \in S_{L'}$ of the masked positions, and each permutation induces a different factorization of the block likelihood via Equation (6). The oracle exhaustively evaluates all $L'!$ permutations per block and selects the one that minimizes the block’s negative log-likelihood:

$$\text{NLL}_{\text{oracle}} = \sum_{b=1}^{L/L'} \min_{\pi \in S_{L'}} \text{NLL}_{\text{DUEL}}^{(b)}(\pi),$$

where $\text{NLL}_{\text{DUEL}}^{(b)}(\pi)$ is the negative log-likelihood contribution of block b under ordering π , computed by running Algorithm 2 with a left-to-right unmasking rule applied to the permuted block positions. Concretely, for each block b :

1. Enumerate all $L'!$ permutations $\pi_1, \dots, \pi_{L'!}$ of the L' positions in block b .
2. For each permutation π_i , run DUEL with the unmasking order defined by π_i : unmask positions in the order $\pi_i(1), \pi_i(2), \dots, \pi_i(L')$, recording the log-probability of each ground-truth token as it is revealed.
3. Select $\pi^* = \arg \min_{\pi_i} \text{NLL}_{\text{DUEL}}^{(b)}(\pi_i)$.

For $L' = 4$, this evaluates $4! = 24$ permutations per block, incurring a $24 \times$ cost relative to a single DUEL evaluation.

Unmasking Rules. In addition to the oracle, we evaluate four standard deterministic rules for comparison: left-to-right, greedy confidence ($k = 1$), probability margin ($k = 1$), and confidence threshold ($\tau = 0.95$). All rules are restricted to block size $L' = 4$; see Section D.2.1 for rule definitions.